Coupled Electron-Ion Monte Carlo Simulation of High Pressure Hydrogen

Carlo Pierleoni
University of L'Aquila, Italy

Collaborators:
- David M. Ceperley, UIUC, Illinois USA
- Kris Delaney, UCSB, California USA
- Markus Holzmann, LPTCM, Paris VI
- Miguel Morales, UIUC, Illinois USA
- Elisa Liberatore, University of Rome, Italy
- Eric Schwegler, LLNL, USA

Acknowledgments:
- INFM and PRIN 2001-2003-2007 for financial support
- NCSA-ORNL (USA), CINECA (Italy) for computer time

Motivation: astrophysics

- Hydrogen is the most abundant element in nature (~90%) in particular in the giant planets of the solar system (Jupiter, Saturn, Uranus, Neptune) and in extrasolar planets recently discovered.
- Other elements in these planets are Helium, Oxigen, inert gases and heavier elements (rocks) in the inner core of the planet.
- Knowledge of the hydrogen and hydrogen-helium Equation of State (EOS) is crucial to make quantitative models for the interior of such planets.
- Those models, refined to match experimental observation, can provide informations about the planet composition, evolution and formation.
- Shock Wave (SW) experimental techniques, developed for Inertial Confinement Fusion research, often can mimic the conditions in the interiors of the planets and provide useful data.

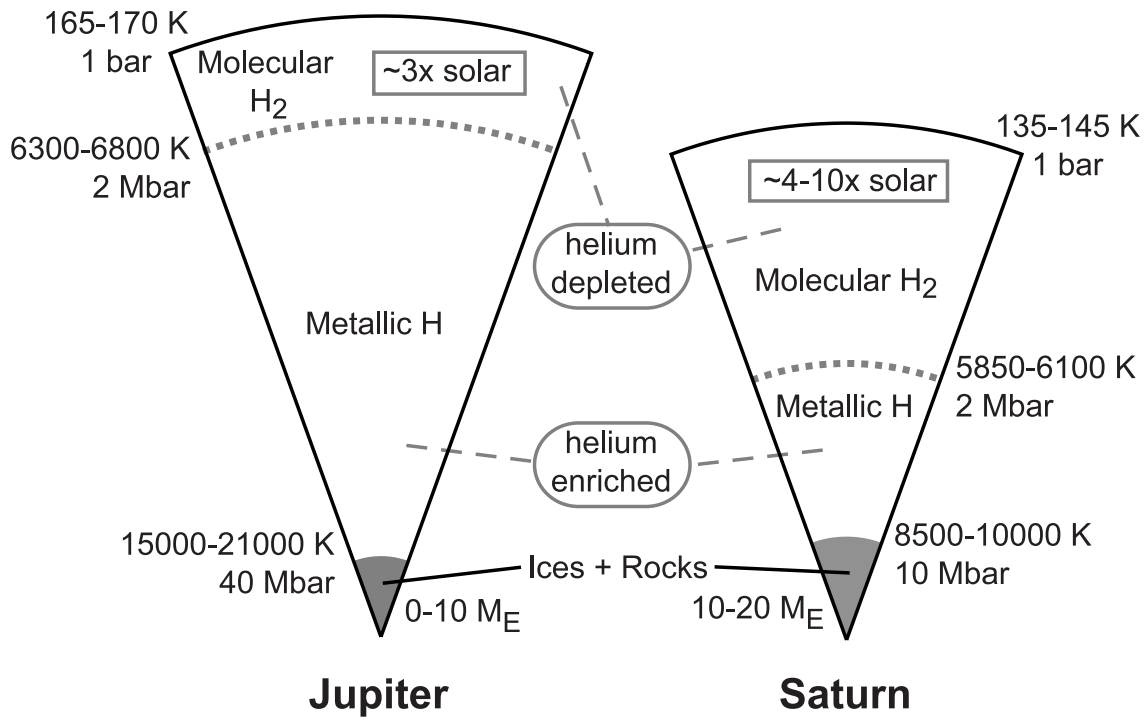

Fig. 1.— Schematic interior structure of Jupiter and Saturn. Pressures and temperature are marked at 1 bar (100 kpa, visible atmosphere), 2 Mbar (200 Gpa, near the molecular-to-metallic transition of hydrogen), and at the top of the heavy element core. Temperatures are especially uncertain, and are taken from Guillot (2005). Approximate atmospheric abundances for "metals" (relative to solar) are shown within the grey box, in the molecular H_2 region. Possible core masses, in $M_\oplus$ (labeled as "M_E") are shown as well (Saumon & Guillot 2004).

Fortney J. J., Astrophysics and Space Science 2006.

Motivation: metallization

- Hydrogen is the simplest element in the periodic table but presents a reach physics.
- At ambient conditions it is molecular and at low temperature its phase diagram is dominated by the orto-para separation (Silvera '80).
- Metallization and molecular dissociation with pressure in the ground state was predicted long ago to be at P~25Gpa (Wigner 1935) but modern experiments up to 350GPa did not found a metallic state (Loubeyre '02).
- The search of metallization in hydrogen has been one of the motivations in developing high pressure Diamond Anvil Cell (DAC) technology.
- Three different insulating molecular crystal phases has been observed so far for increasing pressure.
- The osberved reentrant melting of the molecular crystal and the molecular dissociation-metallization has suggested the existence of a low temperature liquid which separate the molecular crystal from the atomic crystal.

Hydrogen phase diagram

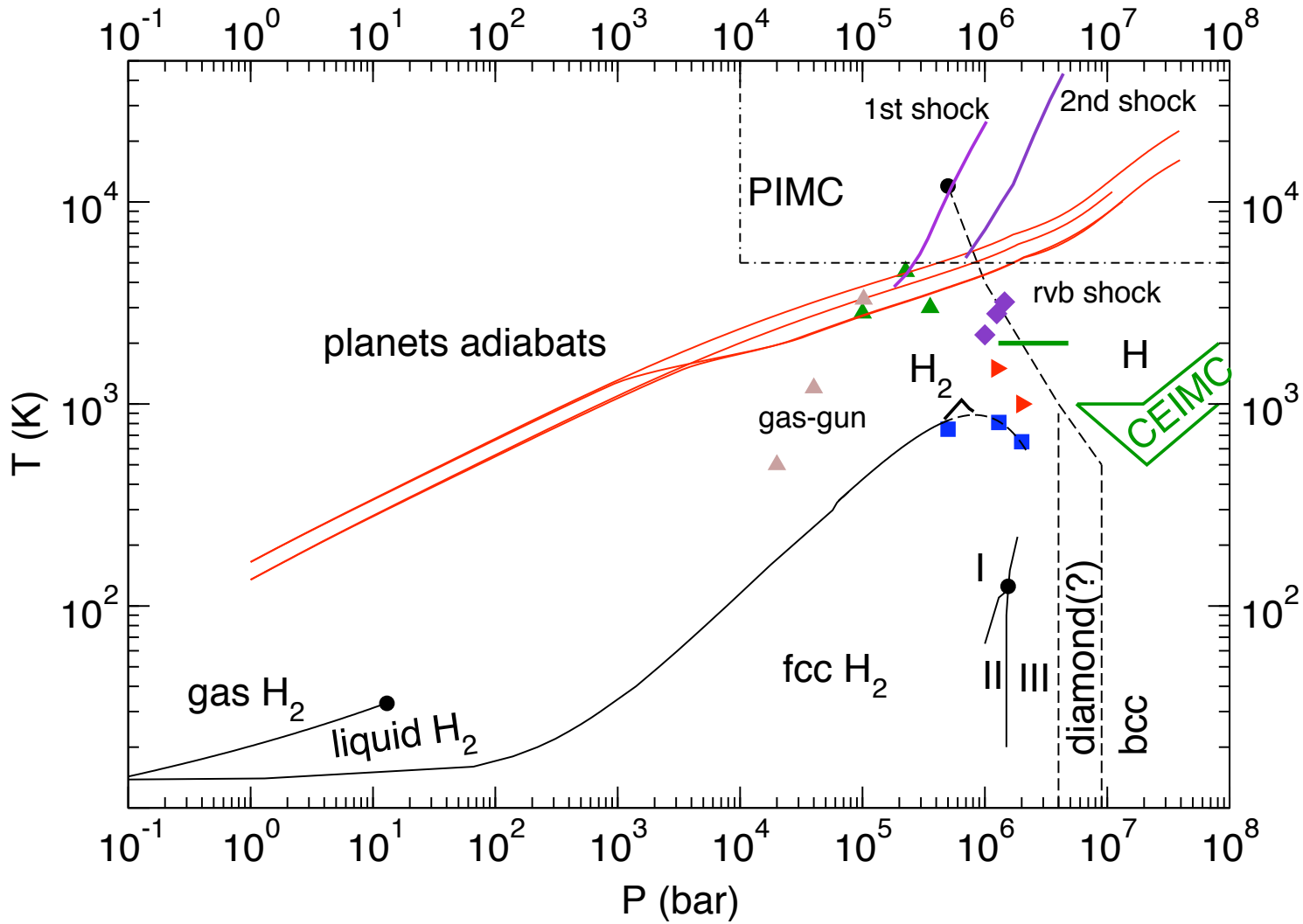

continuous lines (black): experimental phase boundaries
dashed lines: theoretical predictions from various methods
red lines: model adiabats for the interior of the giant planets of the solar system
diamonds: reverberating shock experiment through liquid metallization (Weir et al '96)
1st and 2nd shock: BOMD simulations (Desjarlais '03)
right-triangle: CPMD predictions of molecular dissociation in the liquid phase (Scandolo '03)
shock wave experiment on H_2 and D_2 (Fortov et al. '07)
squares: CPMD predictions of molecular melting line (Bonev et al '04) and experiments (Silvera '08, Eremets '08)

Theoretical predictions

- at T=0K molecular dissociation occurs at r_s=1.31 (DMC, Ceperley Alder PRB '87).
- At the molecular dissociation a diamond structure of protons is predicted. At higher pressure a diamond-bcc transition is expected (DMC, Natoli et al PRL '93).
- several new structures for Phase III at T=0 have been recently proposed (Pickard DFT).
- size effects are crucial in ab-initio simulation to obtain converged results (Brillouine zone sampling in AIMD).
- proton Zero Point Motion is very large and favors isotropic structures (Kitamura et al, Nature 2000, CMPD).
- Predicting metallization requires going beyond DFT-LDA-GGA(Johnson Ashcroft, Nature 2000)
- Most recent prediction (T=0K): Pm~4Mbars within the molecular phase (DFT-Exact-Exchange functional) (Stadele and Martin, PRL 2000).

Motivation: beyond DFT

- Ab-initio simulation methods are the principal source of theoretical information.
- At high temperature, free energy models in the chemical picture have been developed and proved useful to interpret "experimental" results.
- Ab-initio simulations are largely based on Density Functional Theory with approximated functionals (LDA, GGA), in general a good compromise to perform dynamical studies of several hundreds atoms (Car-Parrinello and BO Molecular Dynamics).
- There are cases in which DFT is not accurate enough: Van-der-Waals bonding systems, sp-bonded materials, excitation energies and energy gaps, metallization.
- Quantum Monte Carlo (QMC) provides in general more accurate electronic energies for given ionic positions.

Motivation: beyond DFT

- Can we devise an efficient method to exploit the accuracy of QMC in ab-initio "dynamical" simulation of condensed systems?
- Previous attempts
  - Diffusion Monte Carlo for electrons and nuclei (Ceperley-Alder 1987)
    - temperature effects are absent
    - time scale separation problem (already for hydrogen)
  - Restricted Path Integral Monte Carlo (RPIMC) (Pierleoni, Ceperley et al, 1994, Militzer-Ceperley 1999)
    - electrons and nuclei are at finite temperature
    - sampling problem at low temperature ($T < \frac{1}{20} T_F$, T<5000K)
- Coupled Electron-Ion Monte Carlo (CEIMC)
  - Born-Oppenheimer separation of time scales: ground state electrons, finite T nuclei
  - bridges the gap between finite T PIMC and ground state DMC.

CEIMC

CEIMC: Metropolis Monte Carlo for finite T ions. The BO energy in the Boltzmann distribution is obtained by a QMC calculation for ground state electrons.

- Finite temperature ions: Noisy Monte Carlo The Penalty Method
- Ground state electrons:
  - Variation Monte Carlo (VMC) & Reptation Quantum Monte Carlo (RQMC)
  - Moving the electrons: the bounce algorithm for RQMC
  - Energy difference methods
  - Twist Average Boundary Conditions (TABC) within CEIMC to minimize electronic finite size effects
- Quantum Protons: Path Integral Monte Carlo (PIMC) within CEIMC

CEIMC: trial functions

- QMC for fermions exploits the fixed node approximation and the accuracy depends on the accuracy of the many body trial wave function.
- Slater-Jastrow form: $\Psi_T(R|S) = \exp\left[-U(R|S)\right] \mathrm{Det}\left(\Sigma^{\uparrow}\right) \mathrm{Det}\left(\Sigma^{\downarrow}\right)$
- U(R|S) is a (two-body + three-body + ...) correlation factor (bosonic).
- Σ is a Slater determinant of single electron orbitals $\theta_k(\vec{x}_i, \sigma_i|S)$
- The nodes are determined by the form of the orbitals only. They are the most important part of the trial function since the nodes are not optimized by projection.
- Hydrogen trial function
  - Single electron orbitals obtained from a band structure (OEP) or LDA (DFT) calculation for each proton configuration.
  - Analytical electron-electron backflow transformation (BF) to improve the nodes [Holzmann, Ceperley, Pierleoni, Esler PRE 68, 046707 (2003)].
  - Analytical form for the two body "pseudopotential" within RPA (Gaskell, 1967)
  - No variational parameters to be optimized at the QMC level
  - early implementation (Metallic): fully analytical form of the trial function [free electron orbitals + (ee+ep) backflow + (2body + 3body) Jastrow]

Hydrogen phase diagram

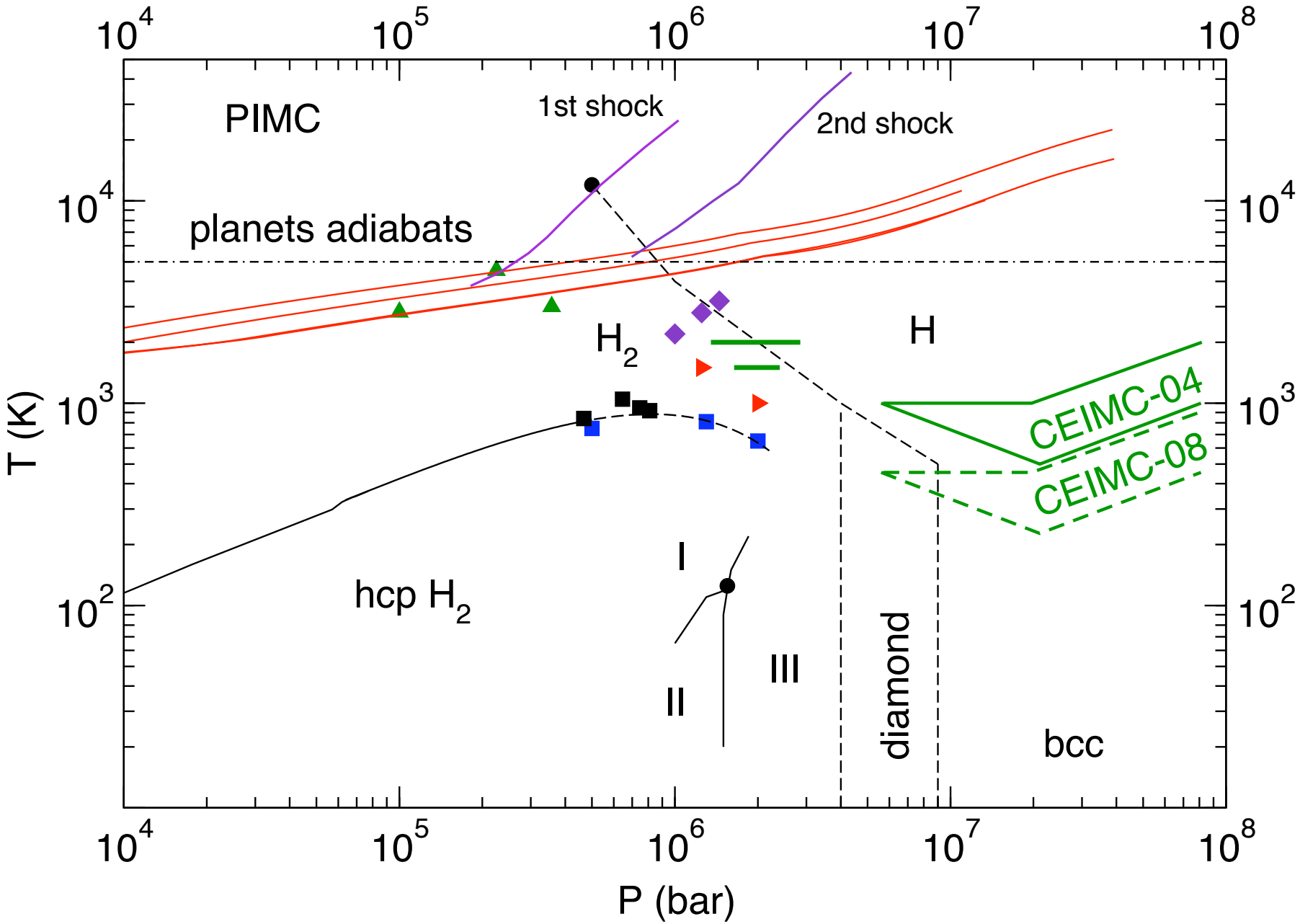

liquid hydrogen

proton-proton pair correlation function

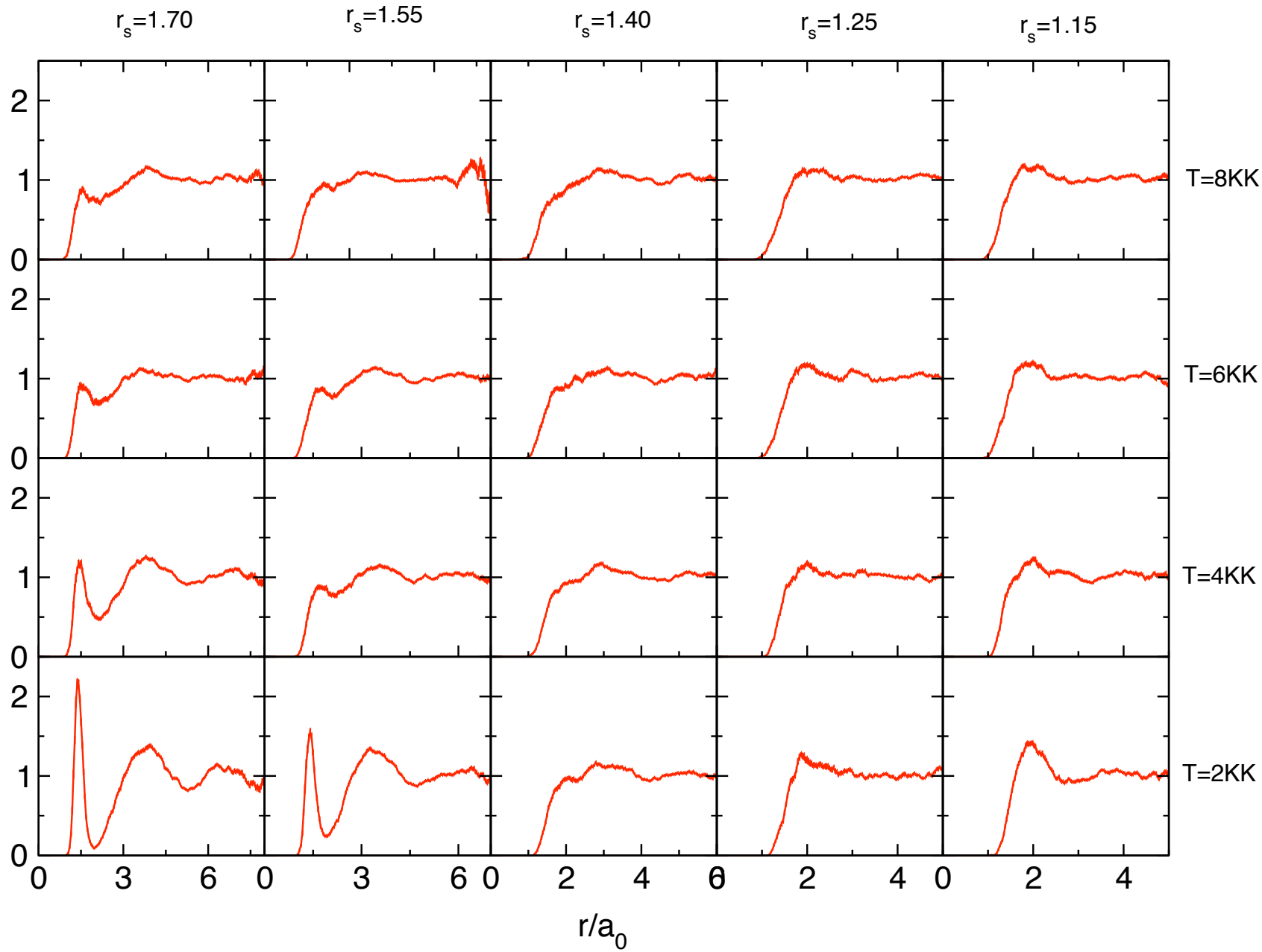

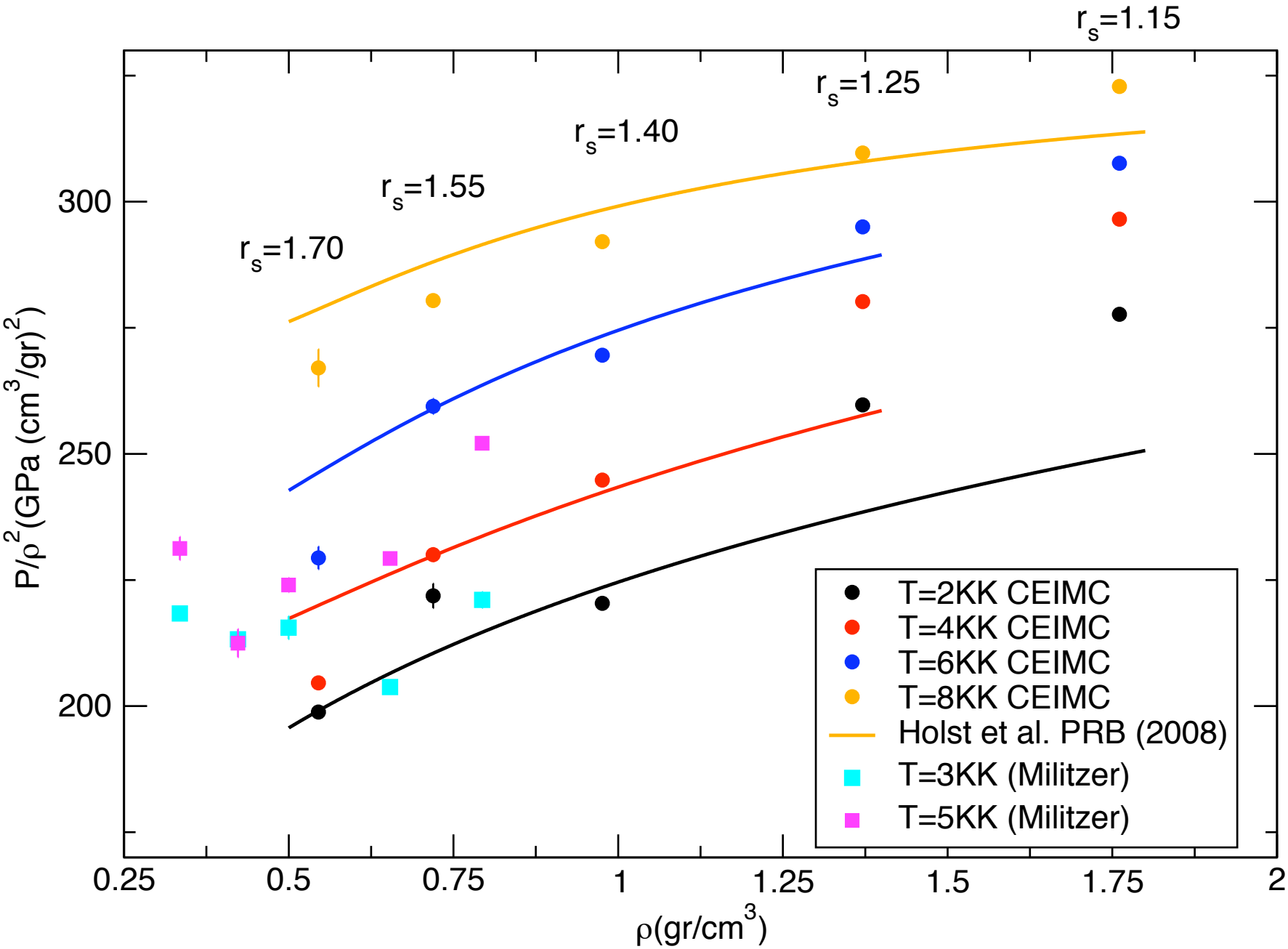
EOS: CEIMC vs BOMD
r_s=1.15
r_s=1.25
r_s=1.40
r_s=1.55
r_s=1.70
300
250
200
P/ρ^2(GPa (cm^3/gr)^2)
0.25
0.5
0.75
1
1.25
1.5
1.75
2
ρ(gr/cm^3)
T=2KK CEIMC
T=4KK CEIMC
T=6KK CEIMC
T=8KK CEIMC
Holst et al. PRB (2008)
T=3KK (Militzer)
T=5KK (Militzer)

Comparison with BOMD-LDA(PBE)

to appear
PRE 2010

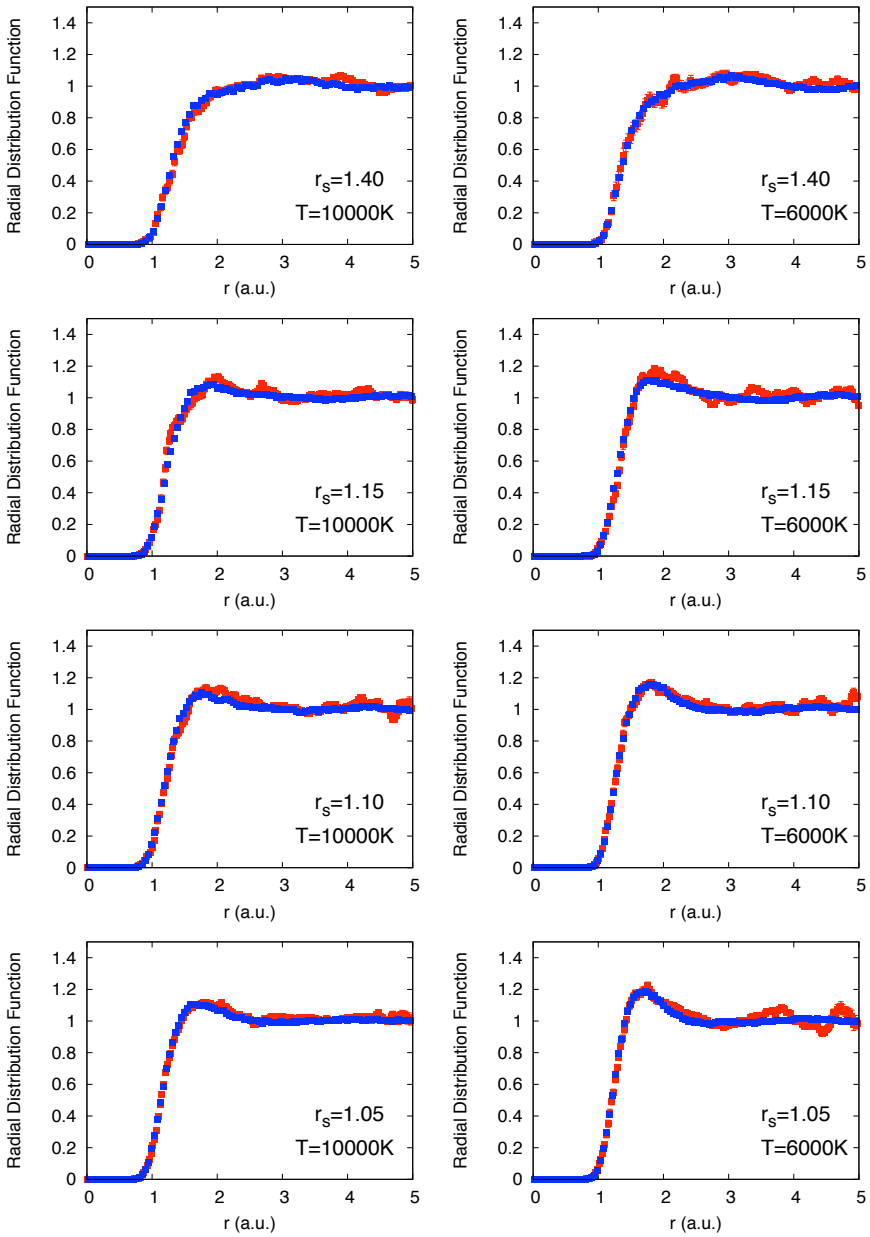

FIG. 4: Comparison of radial distribution functions between BOMD (blue) and CEIMC (red).

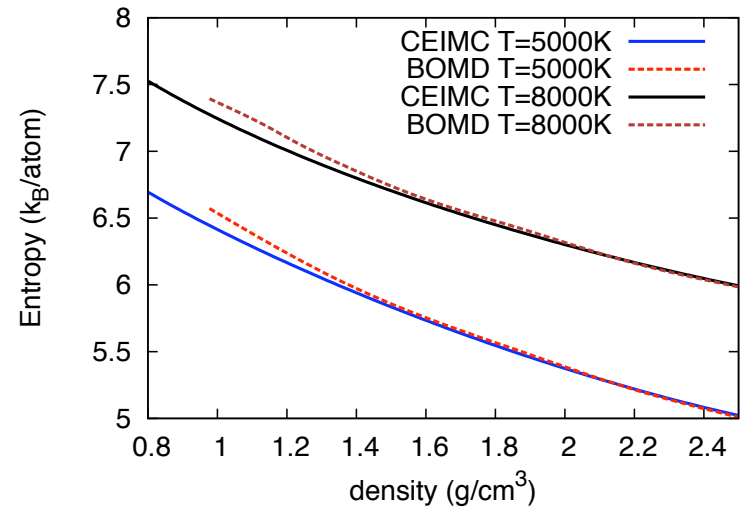

FIG. 5: The entropy/atom at 5000K and 8000K as determined with BOMD and CEIMC.

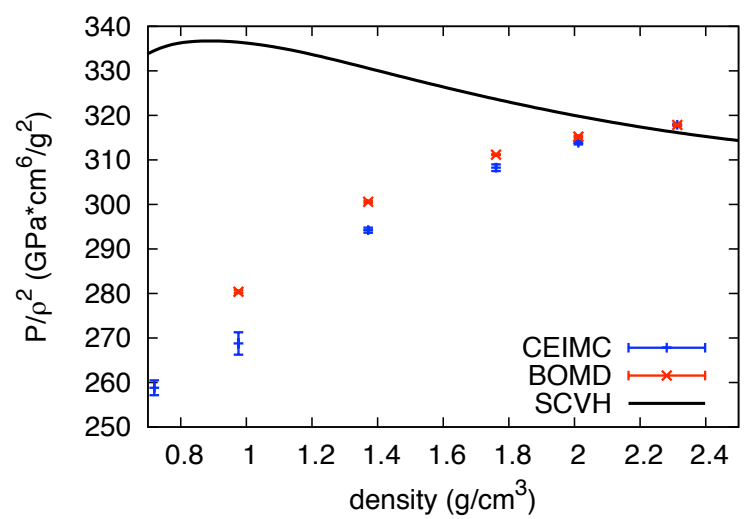

FIG. 6: Comparison of pressure (divided by ρ^2) as a function of density computed with SCVH, BOMD and CEIMC at T=6000 K.

Hydrogen phase diagram

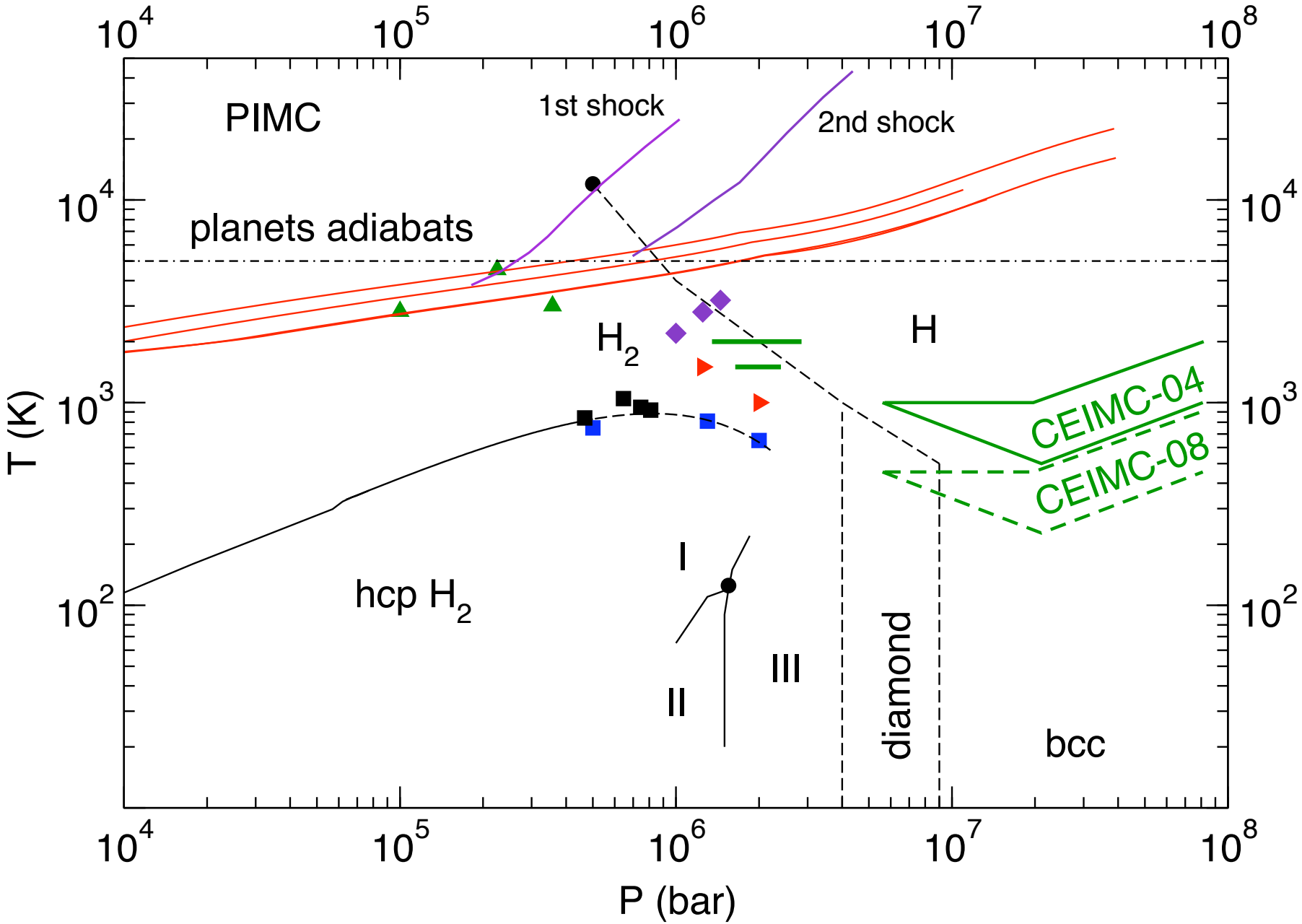

four possible scenarios

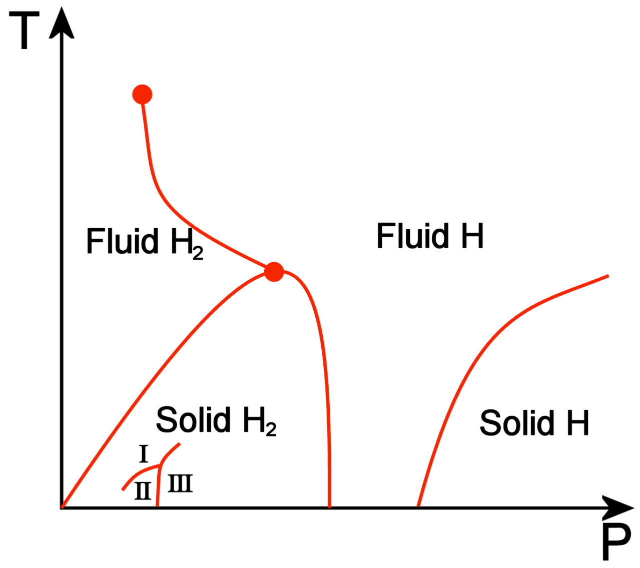

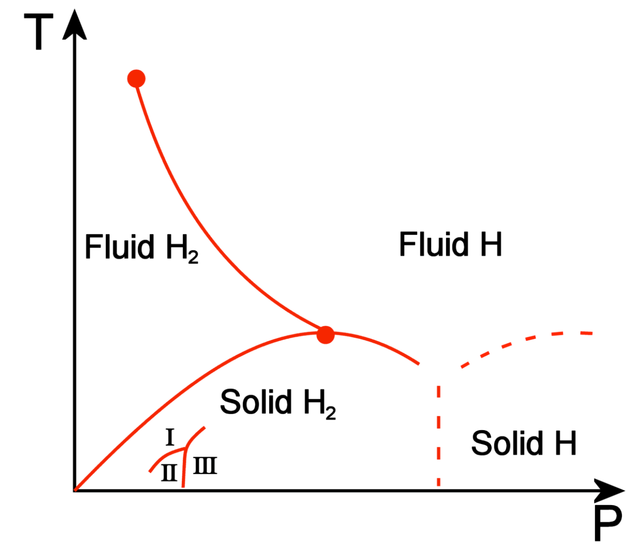

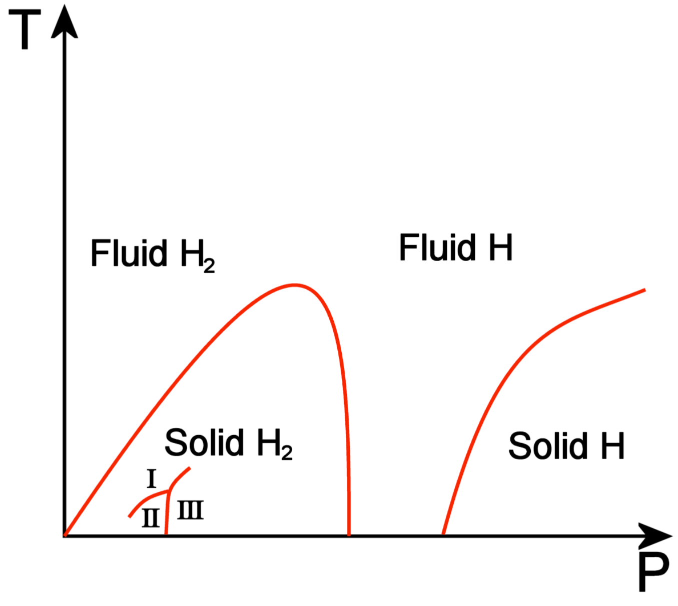

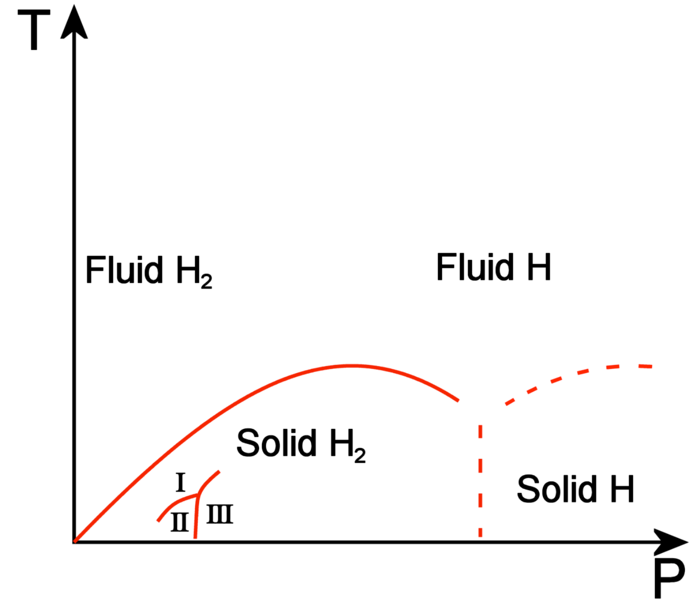

four possible scenarios

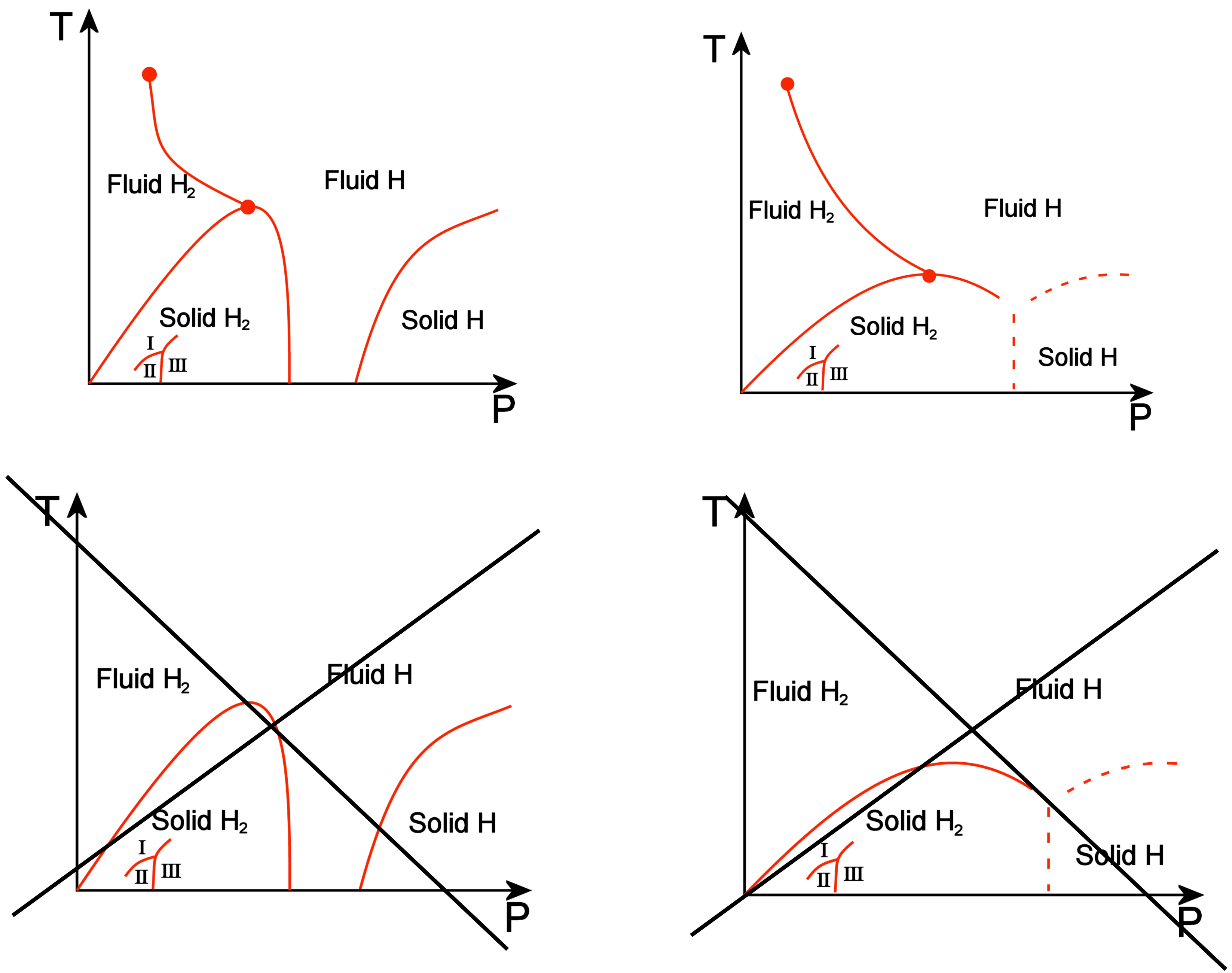

Conclusions

- Hydrogen remains a very interesting system with many open questions in its high pressure regime
  - the existence of a low temperature liquid phase
  - the structure of phase III in the insulating molecular crystal
  - the mechanism of metallization at low temperature and its interplay with molecular dissociation and melting

- CEIMC is an efficient method to perform ab-initio simulation with QMC accuracy
- It is unique in its ability to treat quantum protons without a major computational bottleneck
- It is the obvious method to study hydrogen at intermediate temperature (T>200K)

- In progress:
  - quantum protons effects on the molecular dissociation in the liquid
  - melting of the mono-atomic solid
  - melting of the molecular crystal
  - EOS of hydrogen-helium mixtures

Related Publications

(1) D.M. Ceperley, M. Dewing and C. Pierleoni ``The coupled Electronic-Ionic Monte Carlo simulation method", *Lecture Notes in Physics*, **605**, pp 473-499 (2002).
(2) M. Holzmann., D.M.Ceperley, C. Pierleoni and K. Esler ,``Backflow correlation in the electron gas and metallic hydrogen", *Phys. Rev. E* **68**, 046707 (2003).
(3) C. Pierleoni, D.M. Ceperley and M. Holzmann,``Coupled Electron-Ion Monte Carlo Calculations of Dense Metallic Hydrogen", *Phys. Rev. Lett.* **93**, 146402 (2004).
(4) C. Pierleoni and D.M. Ceperley: ``Computational Methods in Coupled Electron-Ion Monte Carlo", *CHEMPHYSCHEM* **6**, 1872-1878 (2005).
(5) C. Pierleoni and D.M. Ceperley: ``The coupled Electron-Ion Monte Carlo method", *Lecture Notes in Physics*, **703**, 641-683 (2006).
(6) K. Delenay, C. Pierleoni and D.M. Ceperley: ``Quantum Monte Carlo Simulation of the High-Pressure Molecular-Atomic Crossover in Fluid Hydrogen", *Phys. Rev. Letts.* **97**, 235702 (2006).
(7) C. Pierleoni, K. Delaney, M. A. Morales,D.M. Ceperley and M. Holzmann, ``Trial wave functions for high pressure metallic hydrogen", *Comp. Phys. Comm.* **179**, 89 (2008).
(8) M.A. Morales, C. Pierleoni and D.M. Ceperley,"Equation of state of metallic hydrogen from Coupled Electron-Ion Monte Carlo simulations, to appear, PRE 2010
(9) M.A. Morales, C. Pierleoni, E. Schwegler and D.M. Ceperley,"Evidence of the plasma phase transition in high pressure hydrogen from ab-initio simulations", in preparation.

Metallization of Fluid Molecular Hydrogen at 140 GPa (1.4 Mbar)

S. T. Weir, A. C. Mitchell, and W. J. Nellis

Lawrence Livermore National Laboratory, University of California, Livermore, California 94550

(Received 28 August 1995)

Electrical resistivities were measured for liquid H_2 and D_2 shock compressed to pressures of 93–180 GPa (0.93–1.8 Mbar). Calculated densities and temperatures were in the range 0.28–0.36 mol/cm^3 and 2200–4400 K. Resistivity decreases almost 4 orders of magnitude from 93 to 140 GPa and is essentially constant at a value typical of a liquid metal from 140 to 180 GPa. The data are interpreted in terms of a continuous transition from a semiconducting to metallic diatomic fluid at 140 GPa and 3000 K.

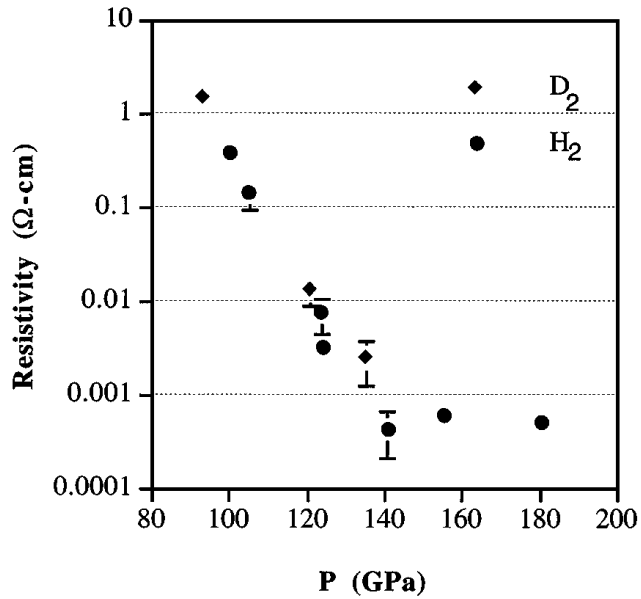

FIG. 1. Electrical resistivity vs pressure for fluid hydrogen and deuterium. The saturation resistivity of 500 $\mu\Omega$ cm above 140 GPa is that of the metallic fluid. Theoretical predictions of this resistivity are a factor of 100 smaller (Refs. [33] and [34]).

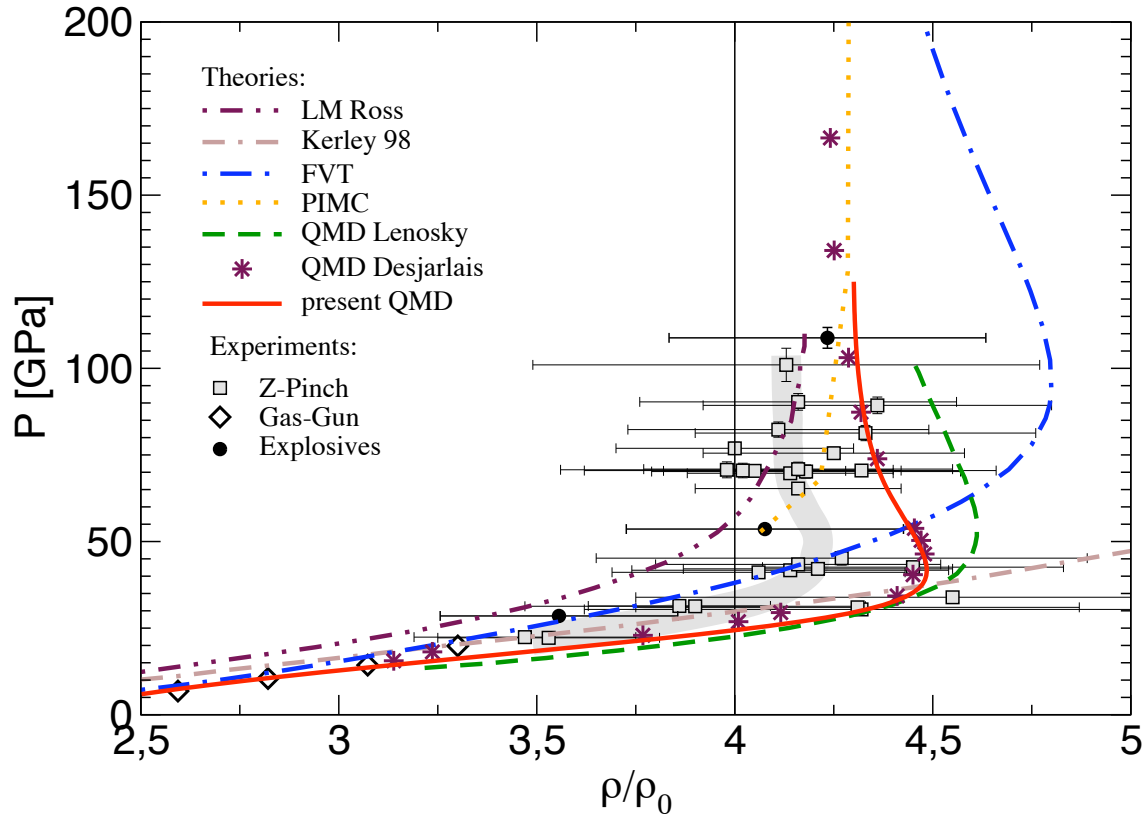

FIG. 5: Principal Hugoniot curve for hydrogen. The results of this work (solid line) are compared with previous QMD results of Lenosky *et al.*[50] (dashed) and Desjarlais[22] (stars), PIMC simulations[54] (dotted), the linear mixing model of Ross[52] (dot-dash-dashed), the model of Kerley[53] (dot-dot-dashed) and the chemical model FVT[42] (dot-dashed). Experiments: Gas gun[48] (diamonds), Sandia Z machine[8] (grey squares; grey line: running average through the u_s-u_p data), high explosives[49] (black circles).

From: Holst, Redmer and Desjarlais, arXiv:0710.1006v1

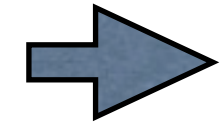

Liquid–liquid phase transition in compressed hydrogen from first-principles simulations

Sandro Scandolo*

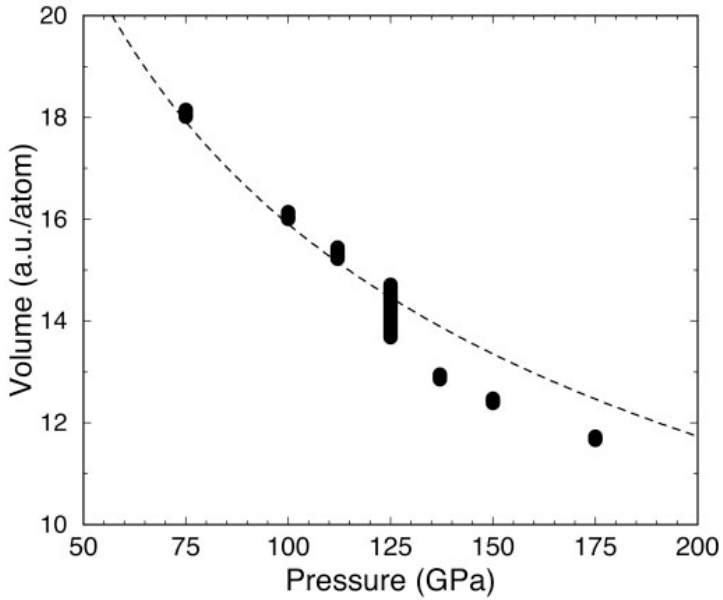

Fig. 1. Calculated volumes for liquid hydrogen at 1,500 K (bars; their size gives the error). The anomalous error bar at 125 GPa is discussed in the text. The dashed line indicates the experimental volume at 300 K (23).

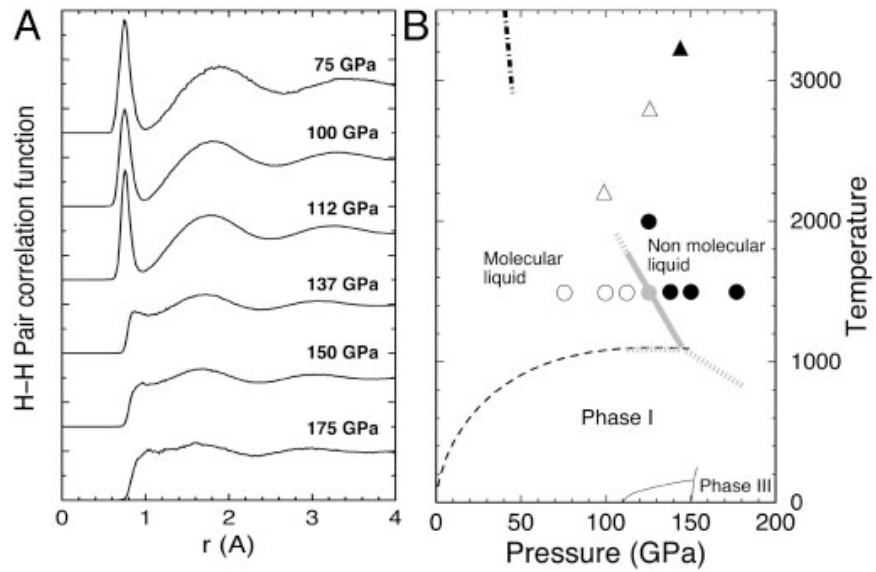

Fig. 2. (*A*) Pair correlation functions of hydrogen at 1,500 K and the pressures indicated. (*B*) Sketch of the hydrogen phase diagram. Circles indicate points where simulations were performed; ○ correspond to points where the system was found to be molecular (nonmolecular points are indicated by ●). Triangles indicate shock-wave points from ref. 2. A continuous transition from insulating (△) to metal (▲) behavior was observed. The dashed line is an extrapolation of the melting line (7). The dash-dotted line is an extrapolation of the first-order transition line predicted by quantum Monte Carlo simulations with free-particle nodes for the electronic wave function (24). Gray lines indicate suggested phase boundaries.

CPMD at constant pressure (Parrinello-Rahman)

Phase Transition in a Strongly Nonideal Deuterium Plasma Generated by Quasi-Isentropical Compression at Megabar Pressures

V. E. Fortov,[1] R. I. Ilkaev,[2] V. A. Arinin,[2] V. V. Burtzev,[2] V. A. Golubev,[2] I. L. Iosilevskiy,[4] V. V. Khrustalev,[2] A. L. Mikhailov,[2] M. A. Mochalov,[2] V. Ya. Ternovoi,[3] and M. V. Zhernokletov[2]

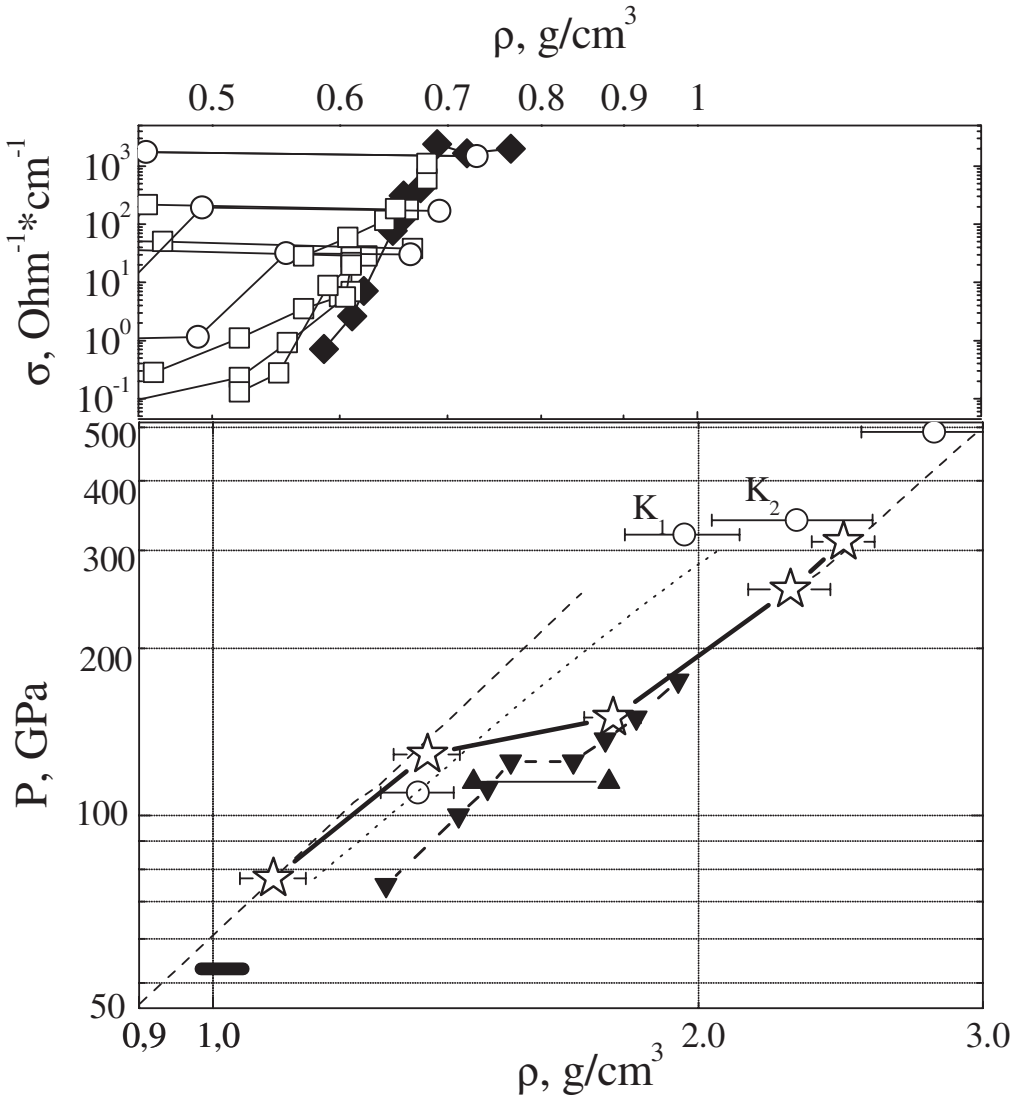

FIG. 4. Isentropic compression of deuterium. Comparison of

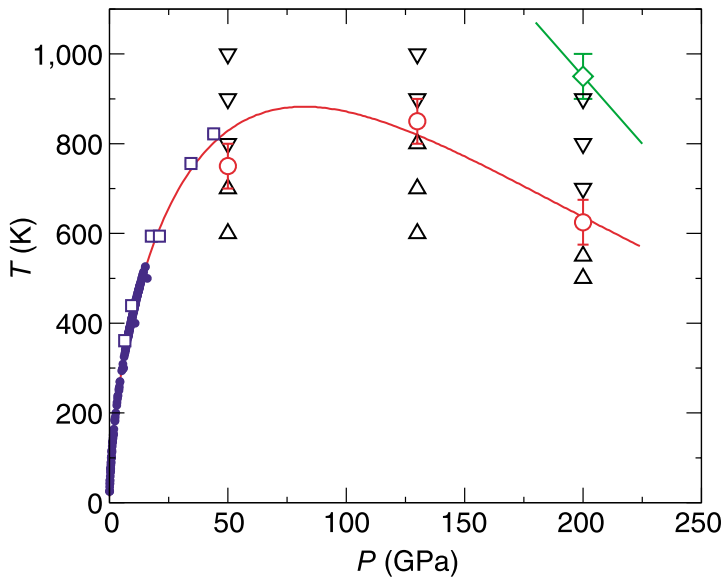

Figure 2 Melt curve of hydrogen predicted from first-principles MD. The filled circles are experimental data from refs 6 and 7 and references therein, and the open squares are measurements from ref. 8. Triangles indicate two-phase simulations where solidification (up) or melting (down) have been observed, and bracketed melting temperatures (T_m) are represented by open circles. As the phase boundary is approached, the period of coexistence increases and eventually the outcome becomes dependent on the choice of simulation parameters. This degree of arbitrariness is reflected in the error bars of T_m, which also include the standard deviation of the temperatures collected during the MD simulations. All experimental and theoretical points are given equal weight and fitted with a Kechin melt equation[30] (solid line in the figure): $T_m = 14.025(1 + P/a)^b \exp(-cP)$ K, where P is in units of GPa, $a = 0.030355$, $b = 0.59991$, and $c = 0.0072997$. The open diamond marks the liquid–liquid transition from molecular to non-molecular fluid at 200 GPa, and the estimated slope of this phase boundary is given by the green line. The error bar on the diamond symbol indicates the hysteresis effects during the simulation of the liquid–liquid transition.

A quantum fluid of metallic hydrogen suggested by first-principles calculations

Stanimir A. Bonev, Eric Schwegler, Tadashi Ogitsu & Giulia Galli

Lawrence Livermore National Laboratory, University of California, Livermore, California 94550, USA

CPMD with two phase simulation

Melting Line of Hydrogen at High Pressures

Shanti Deemyad and Isaac F. Silvera

Lyman Laboratory of Physics, Harvard University, Cambridge, Massachusetts 02138, USA

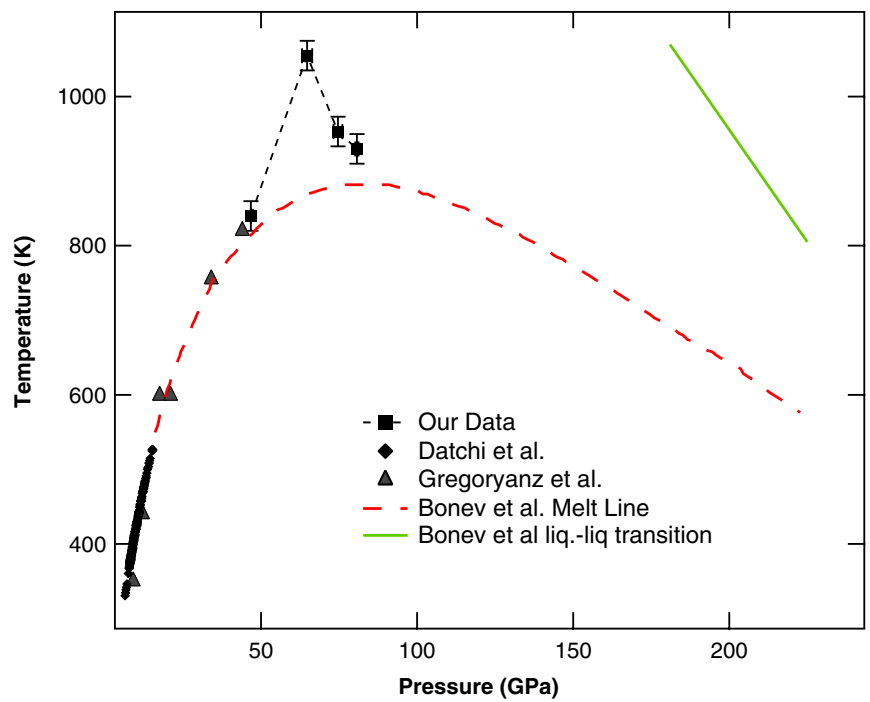

FIG. 4 (color online). The experimental melting line of hydrogen showing our results along with earlier results at lower pressures. Bonev *et al.* fit their theoretical results to a Kechin curve and we show this curve (dashed line). We also show the calculated liquid-liquid phase line for dissociation of hydrogen in the melt.

ISSN 0021-3640, JETP Letters, 2009, Vol. 89, No. 4, pp. 174–179. © Pleiades Publishing, Ltd., 2009.

Evidence of Maximum in the Melting Curve of Hydrogen at Megabar Pressures¶

M. I. Eremets[a] and I. A. Trojan[a, b]

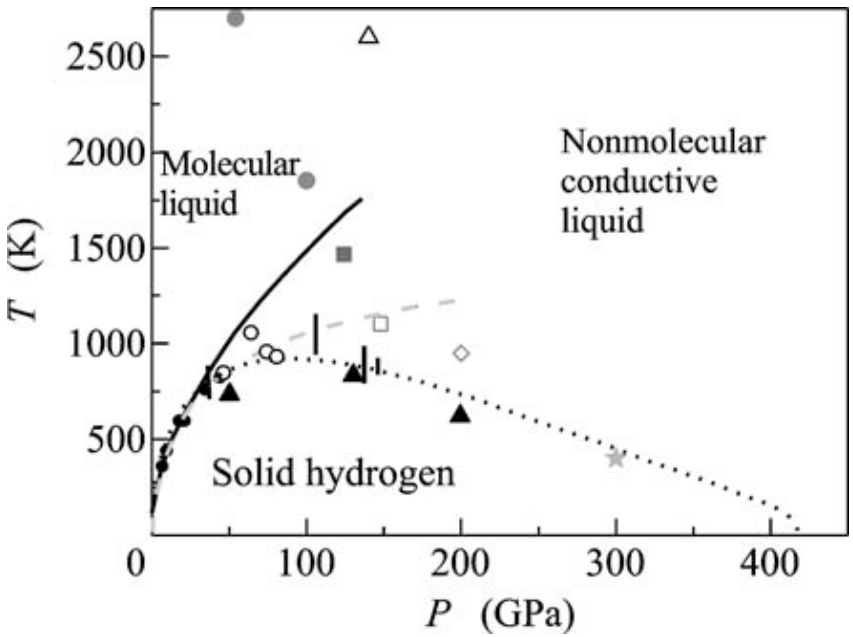

Fig. 1. Phase diagram of hydrogen. Our melting points are shown with black bars. Domain of conductive fluid hydrogen is indicated by the shaded area. The provisional low-temperature boundary of this area is based on calculations (see text for details).

2. EXPERIMENTAL

We performed numerous laser heating runs in four different diamond anvil cells (DACs) loaded cryogenically with hydrogen. Experiments with hydrogen under high-temperature high-pressure conditions pose a number of significant difficulties. The most severe problem is the interaction of hydrogen with diamond anvils: the hot hydrogen easily penetrates diamond anvils causing their breakage to pieces. This inevitably happens at

Structure of phase III of solid hydrogen

CHRIS J. PICKARD[1]* AND RICHARD J. NEEDS[2]

[1]Scottish Universities Physics Alliance, School of Physics and Astronomy, University of St Andrews, St Andrews, Fife KY16 9SS, UK

[2]Theory of Condensed Matter Group, Cavendish Laboratory, Cambridge CB3 0HE, UK

*e-mail: cjp10@st-andrews.ac.uk

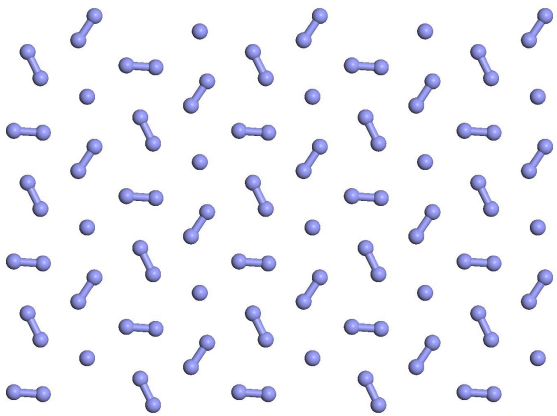

Figure 2: **A layer of the hexagonal $P6_3/m$ structure at 300 GPa.** The layers are stacked in an ABAB fashion, and the primitive unit cell contains 16 atoms which form two types of hydrogen molecule. Three quarters of the molecules lie flat within the plane, and one quarter lie perpendicular to the plane. The centres of the molecules lie on a slightly distorted hexagonal close packed lattice. In this, and Figs. 3, 4, and 5, bonds are indicated between atoms closer than 1.05 Å, and close contacts (pink dashed lines), if they exist, between atoms closer than 1.15 Å.

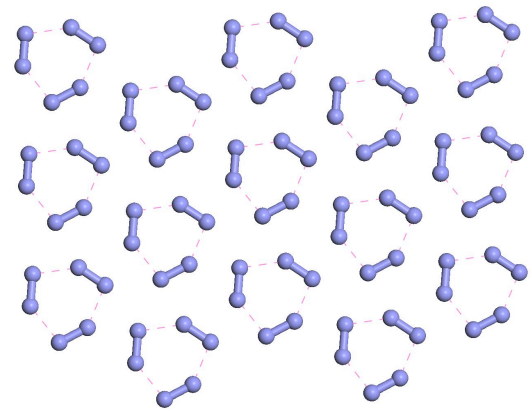

Figure 3: **A layer of the monoclinic $C2/c$ structure at 300 GPa.** The layers are arranged in an ABCDA fashion, and the primitive unit cell contains 24 atoms. Each layer consists of three inequivalent molecules whose axes are nearly parallel to the plane and whose centres form a distorted hexagonal lattice.

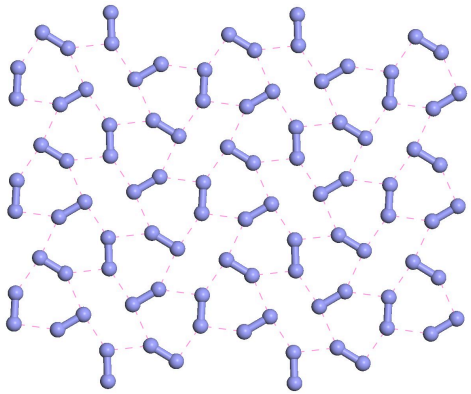

Figure 4: **A layer of the monoclinic $Cmca$-12 structure at 300 GPa.** The layers are arranged in an ABA fashion, and the primitive unit cell contains 12 atoms. The arrangement of the molecules is similar to that in $C2/c$, although the molecules lie flat within the layer and the distortion from hexagonal packing is larger.

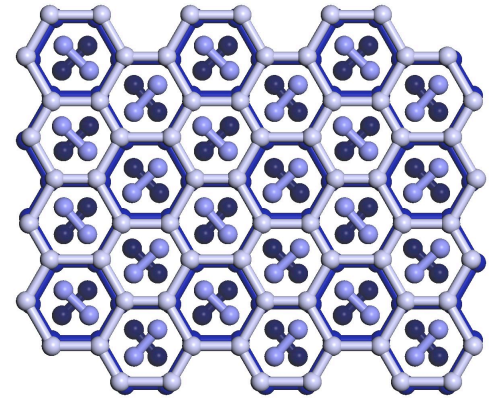

Figure 5: **The $Pbcn$ structure at 300 GPa.** Four layers are depicted, with the colour become successively darker for each deeper layer. On applying further pressure, the bond lengths within the less strongly bonded graphene-like layers become more nearly equal, and the $Ibam$ structure is formed.

Moving the ions

- In Metropolis MC we generate a Markov chain of ionic states S distributed according to Boltzmann

$$P(S) \propto \exp(-\beta E_{BO}(S))$$

$E_{BO}(S) =$ Born-Oppenheimer energy for the configuration S.

- Given an initial state S we propose a trial state S' with probability

$$T(S \rightarrow S') = T(S' \rightarrow S)$$

and we accept the move with probability

$$A(S \rightarrow S') = min\left[1, \exp\left\{-\beta[E_{BO}(S') - E_{BO}(S)]\right\}\right]$$

- After a finite number of moves the Markov chain is distributed with Boltzmann (if ergodicity holds).

- But $E_{BO}(S)$ from QMC is noisy $\Rightarrow$ use the penalty method

The Penalty Method

- Assume mean value and variance of the energy difference over the noise distribution $P(\delta|S,S')$ exist

$$\begin{aligned} \beta[E_{BO}(S') - E_{BO}(S)] &= <\delta(S,S')>=\Delta(S,S') \\ <(\delta-\Delta)^2> &= \sigma^2(S,S') \end{aligned}$$

We want to find the new acceptance probability $a(S \to S')$ such that we satisfy detailed balance on average:

$$T(S \to S') < a(S \to S') >= T(S' \to S) < a(S' \to S) > \exp[-\beta\Delta(S,S')]$$

$$< a(S \to S') >= \int_{-\infty}^{\infty} d\delta P(\delta|S,S') a(\delta|S,S')$$

Under general assumption one can show that

$$a(\delta|\sigma) = min\left[1, \exp\left(-\delta - \frac{\sigma^2}{2}\right)\right]$$

- **The noise always causes extra rejection !**

- In few simple examples the optimal noise level was found to be $s^2 = \sigma^2/n \approx 1$.
  In CEIMC other constraints imposes the noise level but as a rule of thumb we always try to stay around 1.
- $\sigma^2 \sim T^{-2}$: lowering the temperature requires smaller noise level, i.e. longer electronic runs

JOURNAL OF CHEMICAL PHYSICS VOLUME 110, NUMBER 20 22 MAY 1999

The penalty method for random walks with uncertain energies

D. M. Ceperley and M. Dewing
Department of Physics and NCSA, University of Illinois at Urbana-Champaign, Urbana, Illinois 61801

Two level sampling

Since the electronic part is much more expensive than computing any classical effective potential, in CEIMC we can use two level Metropolis sampling to improve the efficiency. Suppose $V_{cl}(S)$ is a reasonable proton-proton potential. The equilibrium distribution can be written as:

$$P(S) \propto e^{-\beta[E_{BO}(S)-V_{cl}(S)]} e^{-\beta V_{cl}(S)} = P_2(S) P_1(S)$$

A trial move is proposed and accepted or rejected based on a classical potential

$$A_1 = \min\left[1, \frac{T(S \to S')}{T(S' \to S)} \exp(-\beta[V_{cl}(S') - V_{cl}(S)])\right]$$

If we accept at the first level, the QMC energy difference is computed and the move accepted with probability

$$A_2 = \min\left[1, \exp(-\beta \Delta E_{BO} - u_B) \exp(\beta[V_{cl}(S') - V_{cl}(S)]\right]$$

where u_B is the noise penalty.

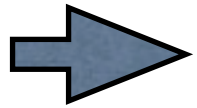

The electronic problem

System of N_p ions and N_e electrons. We need to compute the BO energy

$$E_{BO}(S) = < \Phi_0(S)|\hat{H}|\Phi_0(S) >$$

$|\Phi_0(S) >=$ electronic ground state w.f. for ionic state $S = \{\vec{s}_1, \ldots, \vec{s}_{N_p}\}$.
In configurational space $X = (R, \Sigma) = (\{r_1, \ldots, r_{N_e}\}, \{\sigma_1, \ldots, \sigma_{N_e}\})$

$$E_{BO}(S) = \int dX \, |\Phi_0(X|S)|^2 \, E_L(X|S); \qquad E_L(X|S) = \frac{\hat{H}(R,S)\Phi_0(X|S)}{\Phi_0(X|S)}$$

$$\sigma^2(S) = \int dX \, |\Phi_0(X|S)|^2 \, [(E_L(X|S) - E_{BO}(S)]^2$$

- If $|\Phi_0(S) >$ is an eigenfunction of $\hat{H}$

$$\begin{cases} E_L(X|S) & = E_{BO}(S) \\ \sigma^2(S) & = 0 \end{cases}$$

zero variance principle

Variational Monte Carlo

- The "Variational Theorem": assume a trial wave function for the electrons in the external field of the ions $\Psi_T(X|S)$ and compute the total energy as the average of the local energy $E_L = \Psi_T^{-1} H \Psi_T$

$$E_0 \leq E_T = \frac{< \Psi_T | \hat{H} | \Psi_T >}{< \Psi_T | \Psi_T >} = \frac{\int dX |\Psi_T(X;S)|^2 \Psi_T^{-1}(X;S) \hat{H} \Psi_T(X;S)}{\int dX |\Psi_T(X;S)|^2}$$

- The functional form of the trial wave function must be suitable
  - continuous
  - of proper symmetry
  - normalizable
  - with finite variance (for MC only)
- Parametrized: for a given functional form Ψ_T depends on a number of parameters $\vec{\alpha} = (\alpha_1, \ldots, \alpha_n)$

$$\Psi_T(X|S,\vec{\alpha}) \Longrightarrow E_T(S,\vec{\alpha}) = \langle E_L(X|S,\vec{\alpha}) \rangle$$

Variational Monte Carlo

1. Since $|\Psi_T|^2 \geq 0$, VMC uses Metropolis MC to sample $P(X|S,\alpha) = |\Psi_T|^2 / \int dr |\Psi_T|^2$.
2. take averages of the local energy and the variance
3. optimize over $\{\alpha_i\}$ by minimizing energy and/or variance
4. repeat until convergence is reached

- in CEIMC VMC-optimization should be done for each protonic configuration: major bottleneck for the method
- possible solutions
  - use an automatic optimization method such as Projection MC
  - in special cases use trial wave functions without variational parameters (mono-atomic metallic hydrogen)

Reptation QMC

Assume a trial state $|\Psi_T>$

$$|\Psi_T> = \sum_i c_i \ |\Phi_i> \longleftarrow \text{eigenstates of } \hat{H}$$

$$|\Psi(t)> \equiv e^{-t\hat{H}}|\Psi_T> = \sum_i c_i e^{-tE_i}|\Phi_i> \Longrightarrow \lim_{t\to\infty} |\Psi(t)> \propto |\Phi_0>$$

$$E_0 = \frac{<\Phi_0|\hat{H}|\Phi_0>}{<\Phi_0|\Phi_0>} = \lim_{t\to\infty} \left\{ E(t) = \frac{<\Psi(t/2)|\hat{H}|\Psi(t/2)>}{<\Psi(t/2)|\Psi(t/2)>} = \frac{<\Psi_T|e^{-\frac{t}{2}\hat{H}}\hat{H}e^{-\frac{t}{2}\hat{H}}|\Psi_T>}{<\Psi_T|e^{-t\hat{H}}|\Psi_T>} \right\}$$

Define the generating function of the moments

$$Z(t) = <\Psi_T|e^{-t\hat{H}}|\Psi_T> \Longrightarrow \begin{cases} E(t) = -\partial_t \log Z(t) = <E_L>_t & \longrightarrow E_0 \\ & t \to \infty \\ \sigma^2(t) = \partial_t^2 \log Z(t) = -\partial_t E(t) > 0 & \longrightarrow 0 \end{cases}$$

- The energy converges monotonously from above ($\partial_t E(t) \leqslant 0$)
- At any finite time t, $E(t)$ is a variational upper bound to E_0: $E(t) \geqslant E_0$

Reptation QMC

In configuration space

$$Z(t) = \int dR dR' < \Psi_T | R > \rho(R, R', t) < R' | \Psi_T >$$

$\rho(R, R', t) =< R|e^{-t\hat{H}}|R' >$ is the thermal density matrix at inverse temperature t.

Factorization ($t = M\tau$) $\Longrightarrow$ path integral

$$\rho(R, R', t) =< R|(e^{-\tau\hat{H}})^M|R' >= \int dR_1 \cdots dR_{M-1} \prod_{k=1}^{M-1} \rho(R_{k-1}, R_k, \tau)$$

$R_0 = R, R_M = R'$ paths boundary conditions in imaginary time

Importance sampling

$$Z(t) = \int dR dR' \Psi_T(R) \left\langle e^{-\int_0^t d\tau E_L(R(\tau))} \right\rangle_{DRW} \Psi_T(R')$$

Summary of FN-RQMC

- Build a path $Q = (R_0, \ldots, R_M)$ for the system of N_e electrons at fixed ionic configuration S.
- Sample the path space according to the distribution

$$\begin{aligned} \mathbf{\Pi(Q|S)} &= \exp\left[- U(R_0|S) - U(R_M|S) - A(Q|S)\right] \\ U(R|S) &= \Re[\ln \Psi_T(R|S)] \\ A(Q|S) &= \text{path action} \end{aligned}$$

- **FN:** check $\Psi_T(R_{k-1})\Psi_T(R_k) > 0$ along the path. Otherwise reject the new path.
- Compute the local energy and the variance at path ends, other properties at the middle:

$$O(t) = \frac{1}{Z(t)} \int dR_1 dR_2 dR_3 \Psi_T^*(R_1)\rho(R_1, R_2|\frac{t}{2}) < R_2|\hat{O}|R_2 > \rho(R_2, R_3|\frac{t}{2})\Psi_T(R_3)$$

no mixed estimators bias!!!

- ensure convergence to the continuum limit ($\tau \rightarrow 0$) and to the ground state ($t \rightarrow \infty$)

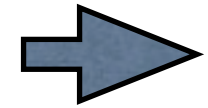

Sampling the electrons

VMC: in classical systems it is usually more efficient to move the particles one at a time by adding a random vector to a particle's coordinate. This remains true in VMC if we can update the Slater determinant efficiently (single row and column updates).
With backflow wave functions we would need to recompute the entire Slater determinant after any single particle move $\Longrightarrow$ global moves.

RQMC: at each move one end of the *many-body polymer* is randomly chosen.
A number of links are cut at the sampled end and added to the opposite end.
Detailed balance is imposed by computing the probability of the reverse move.
Problems: a) the memory of this algorithm in MC step scales as $(\#beads)^2$/acceptance.
b) persistent configurations can appear
Bounce algorithm: we propose to choose at random one end of the chain at the beginning of the calculation and to reverse the growth direction upon rejection only.
It is possible to prove that it samples the correct probability distribution (Pierleoni Ceperley, ChemPhysChem 2005).
Nice scaling of the memory.
No persistent configurations observed.

The bounce algorithm

Bounce algorithm: choose at random one end of the chain at the beginning of the Markov chain and reverse the growth direction upon rejection only. Minimal modification of the algorithm and solve both problems

Proof of the Bounce algorithm:

- enlarge the configurational space $\{Q, d\}$ and define $P(Q, d \to Q', d')$.
- assuming ergodicity, the Markov chain converges to a unique stationary state, $\Upsilon(Q, d)$ solution of the eigenvalue equation:

$$\sum_{Q,d} \Upsilon(Q, d)\, P(Q, d \to Q', d') = \Upsilon(Q', d').$$

- allowed transitions

$$P(Q, d \to Q', d') \neq 0 \Longleftrightarrow \begin{cases} d = d' & , Q \neq Q' \quad \text{accepted move} \\ d' = -d & , Q = Q' \quad \text{rejected move.} \end{cases}$$

- assume $d' = +1$. Since $\Pi(Q)$ does not depend on d

$$\Pi(Q')P(Q', -1 \to Q', 1) + \sum_{Q \neq Q'} \Pi(Q)P(Q, 1 \to Q', 1) = \Pi(Q').$$

The bounce algorithm

- DB $(\Pi(Q)P(Q,1 \to Q',1) = \Pi(Q')P(Q',-1 \to Q,-1))$ provides

$$\Pi(Q')\left[P(Q',-1 \to Q',1) + \sum_{Q} P(Q',-1 \to Q,-1)\right] = \Pi(Q')$$

The term in the bracket exhausts all possibilities for a move from the state $(Q',-1)$, thus it adds to one. Hence $\Pi(Q)$ is a solution and by the theory of Markov chains, it is the unique probability distribution of the stationary state.

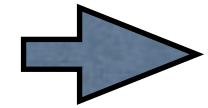

Energy difference method

- In CEIMC we need to evaluate the energy difference between two closeby protonic configurations (S,S').
- Two independent electronic calculations (uncorrelated sampling) is very inefficient for $\Delta E << E$.
- Optimal sampling function: minimizes the variance of the energy difference

$$P(Q|S,S') \propto \left|\Pi(Q|S)(E_S - < E_S >) - \Pi(Q|S')(E_{S'} - < E_{S'} >)\right|$$

  but it requires an estimate of $< E_S >, < E_{S'} >$.
- simpler form: $P(Q|S,S') \propto \Pi(Q|S) + \Pi(Q|S')$
- These two forms have the properties that
  - sample regions of both configuration spaces (S and S')
  - make the energy difference bounded
- compute properties for the system S by reweighting technique (RQMC easier than DMC).

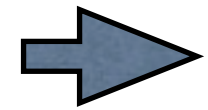

Finite size effects: TABC

- In the metallic systems finite size effects coming from the discrete structure of the Fermi surface are dominant and must be carefully treated.
  The finite size effects can be reduced to the classical $1/N$ behavior averaging over the undetermined phase of the wave function (Li et al. PRE 2001). For periodic systems we have

$$\Psi(\vec{r}_1 + L\hat{\vec{x}}, \vec{r}_2, \cdots) = e^{i\theta_x}\,\Psi(\vec{r}_1, \vec{r}_2, \cdots) \qquad\qquad \theta \in [-\pi, \pi)$$

  TABC:

$$A = \frac{1}{(2\pi)^3}\int_{-\pi}^{\pi} d^3\theta < \Psi_\theta |A| \Psi_\theta >$$

- In practice θ can be chosen on a 3D grid and independent calculations are performed for each grid point.
- (Almost) no extra cost for TABC in CEIMC since we sum over twist angles to reduce the noise.

Finite size effects: TABC

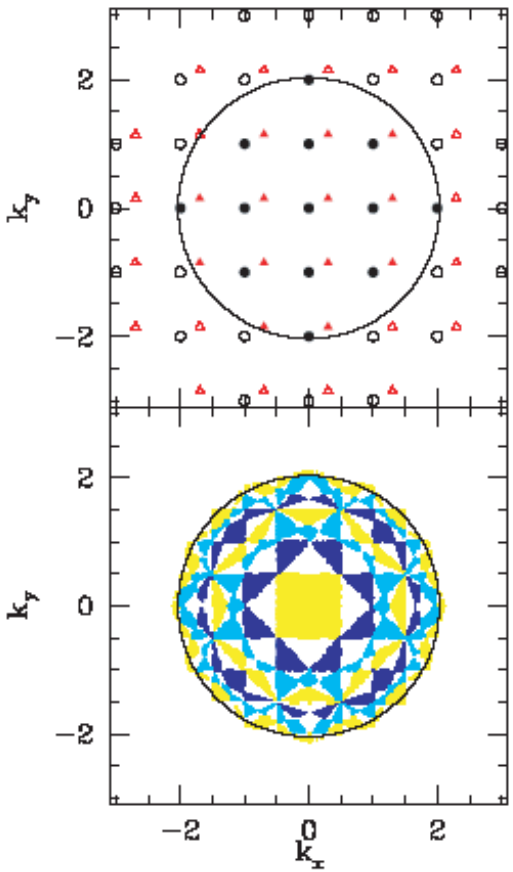

FIG. 1. Momentum distibution for 13 spinless fermions in a 2D square with side $L = 2\pi$. The top panel shows the occupied states (closed symbols) and empty states (open symbols) with zero twist (circles, PBC) and a twist equal to $2\pi(0.3, 0.15)$ (triangles). The circle shows the infinite system fermi surface. The bottom panel shows the occupied states with TABC. The colored regions show the occupied region for the lowest level (middle square), the third level, up to the outermost 13^{th} level.

Lin, Zong, Ceperley PRE 64, 016702 (2001)

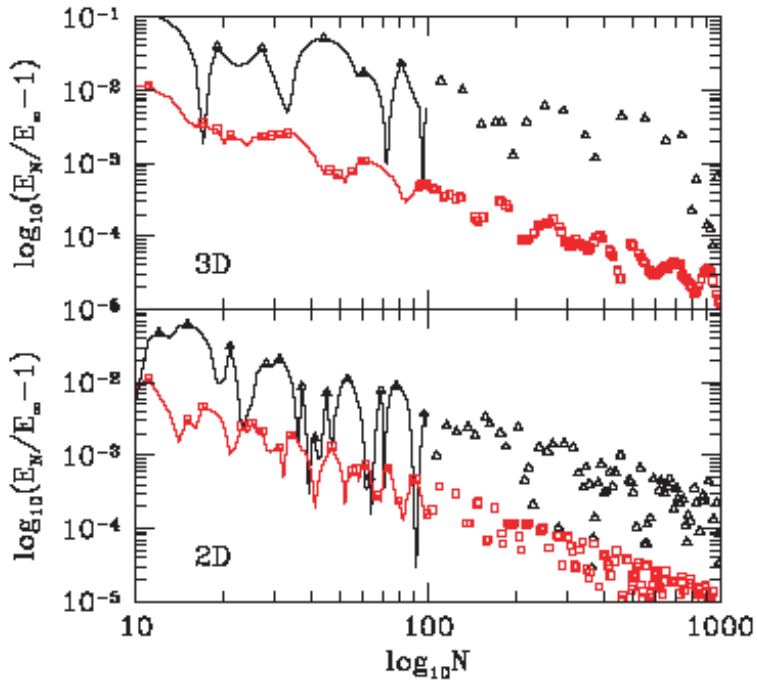

FIG. 2. Relative error of the energy versus number of particles with PBC (△) and TABC (□) in 2D and 3D. The points shown are only those where the relative error has a local maximum. Curves are shown only for $N < 100$.

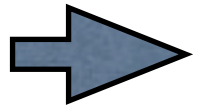

Quantum protons

- By increasing pressure or decreasing temperature, ionic quantum effects start to become relevant. Those effects are important for hydrogen at high pressure.
- Static properties of quantum systems at finite temperature can be obtained with Path Integral Monte Carlo method (PIMC).
  We need to consider the thermal density matrix rather than the classical Boltzmann distribution:

$$\rho_P(S, S'|\beta) =< S|e^{-\beta(K_p+E_{BO})}|S' >$$

  The same formalism as in RQMC applies. However
  1 - β is the physical inverse temperature now.
  2 - to compute averages of diagonal operators we map quantum protons over ring polymers
  3 - we limit to distinguishable particle so far ($T > T_d$), but Bose or Fermi statistics could be considered.
- Factorization $\beta = P\tau_p$ and Trotter break-up
  For efficiency introduce an effective proton-proton potential $\hat{H}_{eff} = \hat{K}_P + \hat{V}_{eff}$

$$\hat{\rho}_P(\tau_p) = e^{-\tau_p[\hat{H}_{eff}+(\hat{E}_{BO}-\hat{V}_{eff})]} \approx e^{-\tau_p\hat{H}_{eff}}e^{-\tau_p[\hat{E}_{BO}-\hat{V}_{eff}]}$$

Quantum protons - 2

- We compute numerically the matrix elements of the effective pair density matrix $\hat{\rho}^{(2)}_{eff}(\tau_p)$ (see lecture notes). The effective N-body density matrix is approximated by

$$< S|\hat{\rho}^{(N)}_{eff}(\tau_p)|S' > \approx \prod_{ij} < s_i, s_j|\hat{\rho}^{(2)}_{eff}(\tau_p)|s_i, s_j > +O(n^3)$$

- We add the remaining term of the original Hamiltonian $(E_{BO} - V_{eff})$ at the level of the primitive approximation.
- With this Trotter break-up we found convergence to the continuum limit ($\tau_p \rightarrow 0$) for $1/\tau_p \geqslant 3000K$ which allows to simulate systems at room temperature with only $M \approx 10$ proton slices (for metallic hydrogen at $r_s = 1$).

Quantum protons - 3

In CEIMC quantum protons are (almost) **for free !**

- Suppose we run classical ions with a given level of noise $(\beta\sigma_{cl})^2$. Consider now representing the ions by P time slices. To have a comparable extra-rejection due to the noise we need a noise level per slice given by: $(\tau_p\sigma_k)^2 \approx (\beta\sigma_{cl})^2/P$ which provides $\sigma_k^2 \approx P\sigma_{cl}^2$. We can allow a noise per time slice P times larger which means considering P times less independent estimates of the energy difference per slice. However we need to run P different calculations, one for each different time slice, so that the amount of computing for a fixed global noise level is the same as for classical ions.
- When using TABC, for any proton time slice we should in principle perform a separate evaluation of the BO energy difference averaging over all twist angles. We have checked that, at each proton step, we can randomly assign a subset of twists at each time slice and get the same results.
- We need to move all slices of all protons together. This limits the length of proton paths, therefore the temperature we can achieve. It is essential to use the best possible Trotter factorization!!

Summary of CEIMC

- Given an initial configuration of the electronic path $Q = \{R_1, \ldots, R_t\}$ and the protonic path $P = \{S_1, \ldots, S_P\}$, propose a trial protonic move P' with a suitable transition probability (depending on the particular system).
- Assign at random an equal number of twist angles to any proton slice and run many independent electronic calculations for each twist angle: ideal for parallel computers !
- Sample the electronic configuration space with the importance sampling distribution depending on both P and P'.
- Use reweighting to compute energy difference Δ and variance σ^2 by averaging results over all twist angles and proton slices
- Performe the Metropolis test with the penalty method
- Compute average quantities for the old protonic configuration P using reweighting.

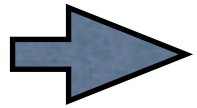

Backflow-3body trial functions

$$\Psi_T(\vec{R}|S) = det(e^{i\vec{k}_i\cdot\vec{x}_j})exp\left(-\sum_{i=1}^{N_e}\left[\frac{1}{2}\sum_{j\neq i}^{N_e}\tilde{u}_{ee}(r_{ij}) - \sum_{j=1}^{N_p}\tilde{u}_{ep}(r_{ij}) - \frac{1}{2}\vec{G}(i)\cdot\vec{G}(i)\right]\right)$$

backflow:

$$\vec{x}_i = \vec{r}_i + \sum_{j\neq i}^{N_e}\eta_{ee}(r_{ij})(\vec{r}_i - \vec{r}_j) + \sum_{j=1}^{N_p}\eta_{ep}(r_{ij})(\vec{r}_i - \vec{r}_j)$$

$$\eta_\alpha(r) = \lambda_b^\alpha exp[-(r/w_b^\alpha)^2]$$

3body:

$$\mathbf{G}(i) = \sum_{j\neq i}^{N_e}\xi_{ee}(r_{ij})(\vec{r}_l - \vec{r}_j) + \sum_{j=1}^{N_p}\xi_{ep}(r_{ij})(\vec{r}_i - \vec{r}_j)$$

$$\tilde{u}_{ee}(r) = u_{ee}(r) - \xi_{ee}^2(r)r^2$$

$$\tilde{u}_{ep}(r) = u_{ep}(r) - \xi_{ep}^2(r)r^2$$

$$\xi(r) = \lambda_T^\alpha exp[-(r/w_T^\alpha)^2]$$

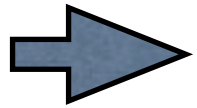

CEIMC: trial functions

- DFT/band orbitals (cusp corrected) + J-RPA + eeBF-A.

  eeBF improves the energy and reduces the variance by two!!!
  (RQMC: Δt=0.01 a.u., T=1.5 a.u.)

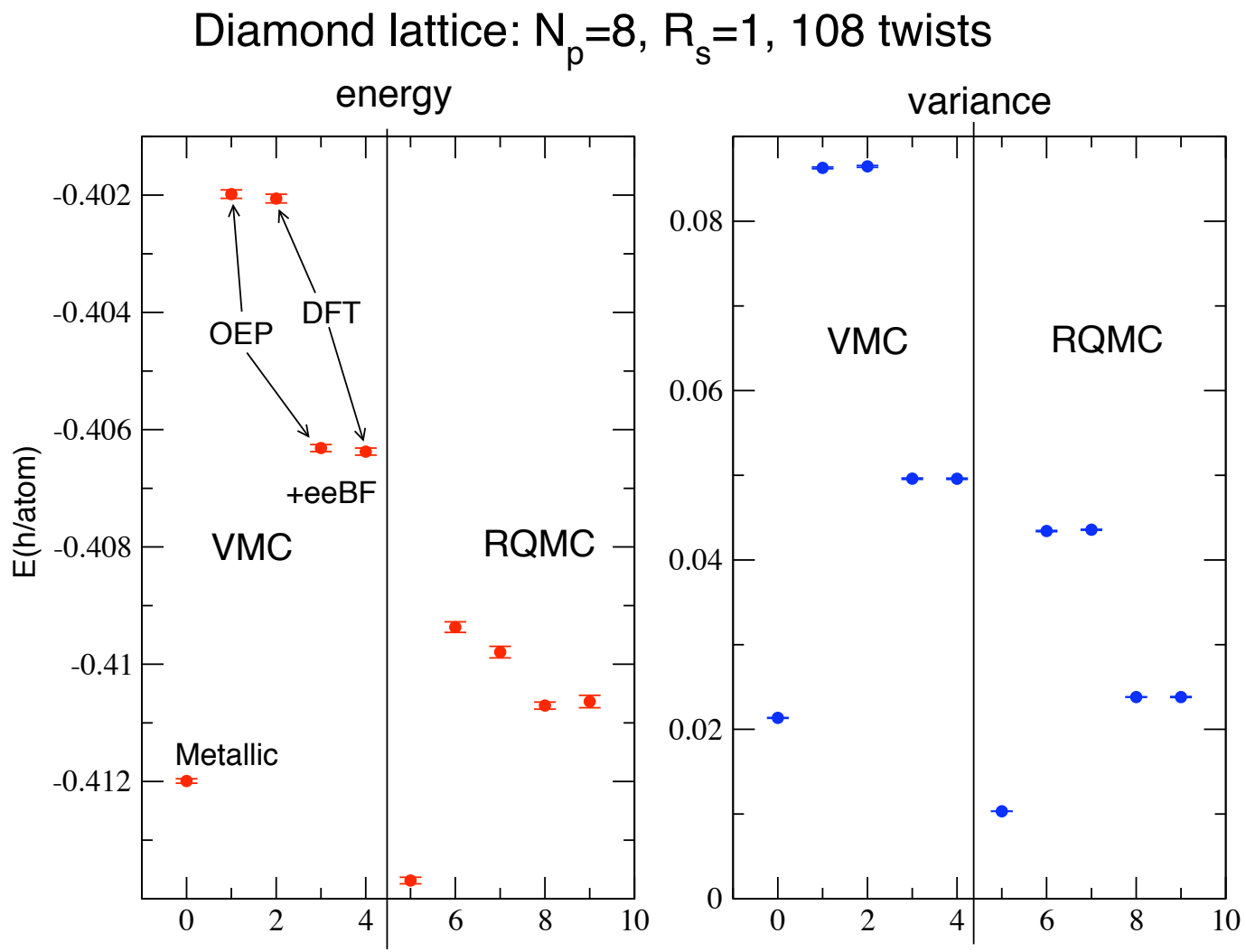

CEIMC: trial functions

R_s=1, N_p=54: Metallic vs DFTBF trial functions

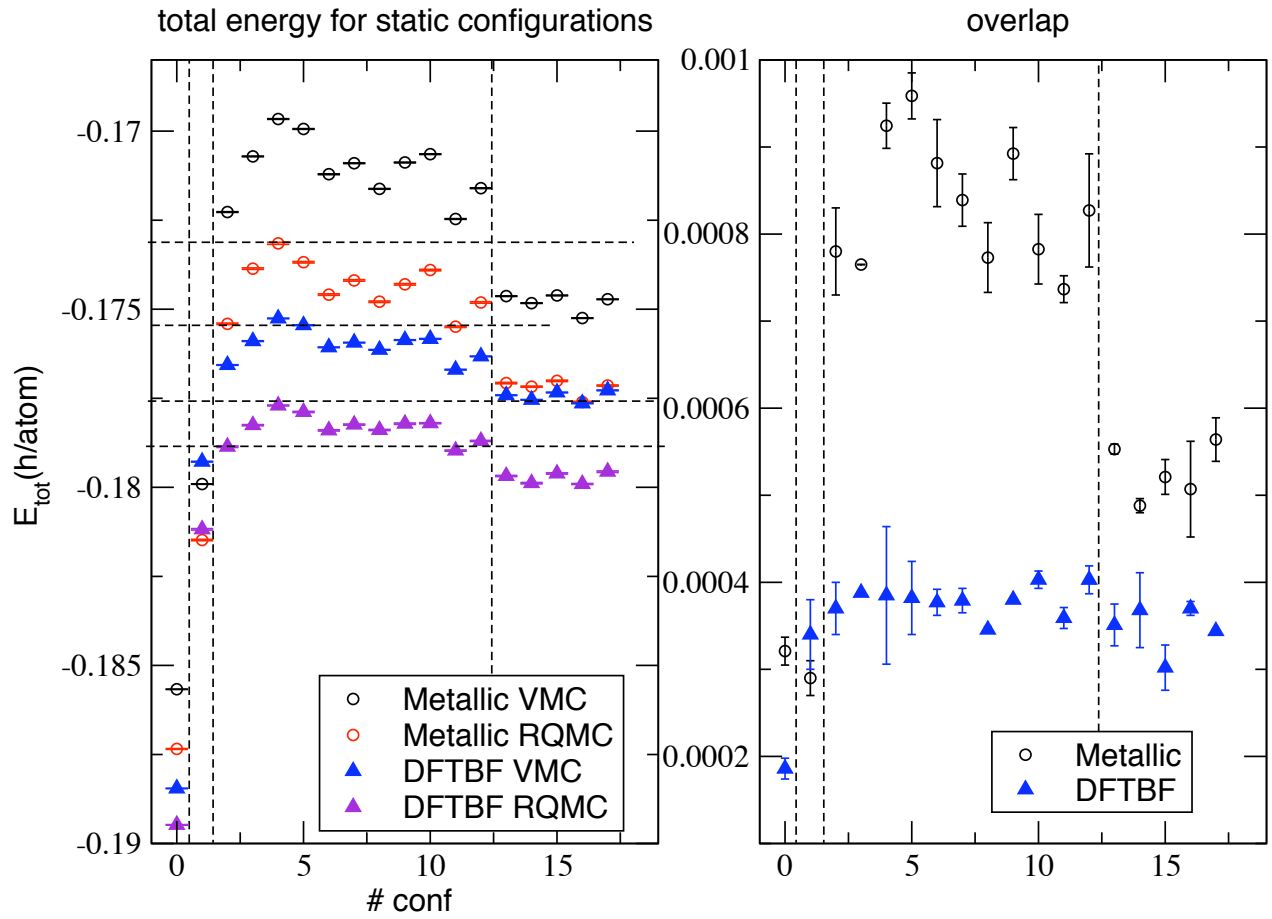

$E_{DFTBF} < E_{Met}$; $O_{DFTBF} < O_{Met}$

Energy dispersions (mH/at)

- Δ_{dftbf}=2.54(4); Δ_{met}=4.68(4)
- Δ_{rqmc}=2.54(4); Δ_{vmc}=2.88(4)

almost a factor of 2!

$\Delta_{vmc}/\Delta_{rqmc} \sim 1.13$

Metallic liquid hydrogen: Rs=1, T=1000K

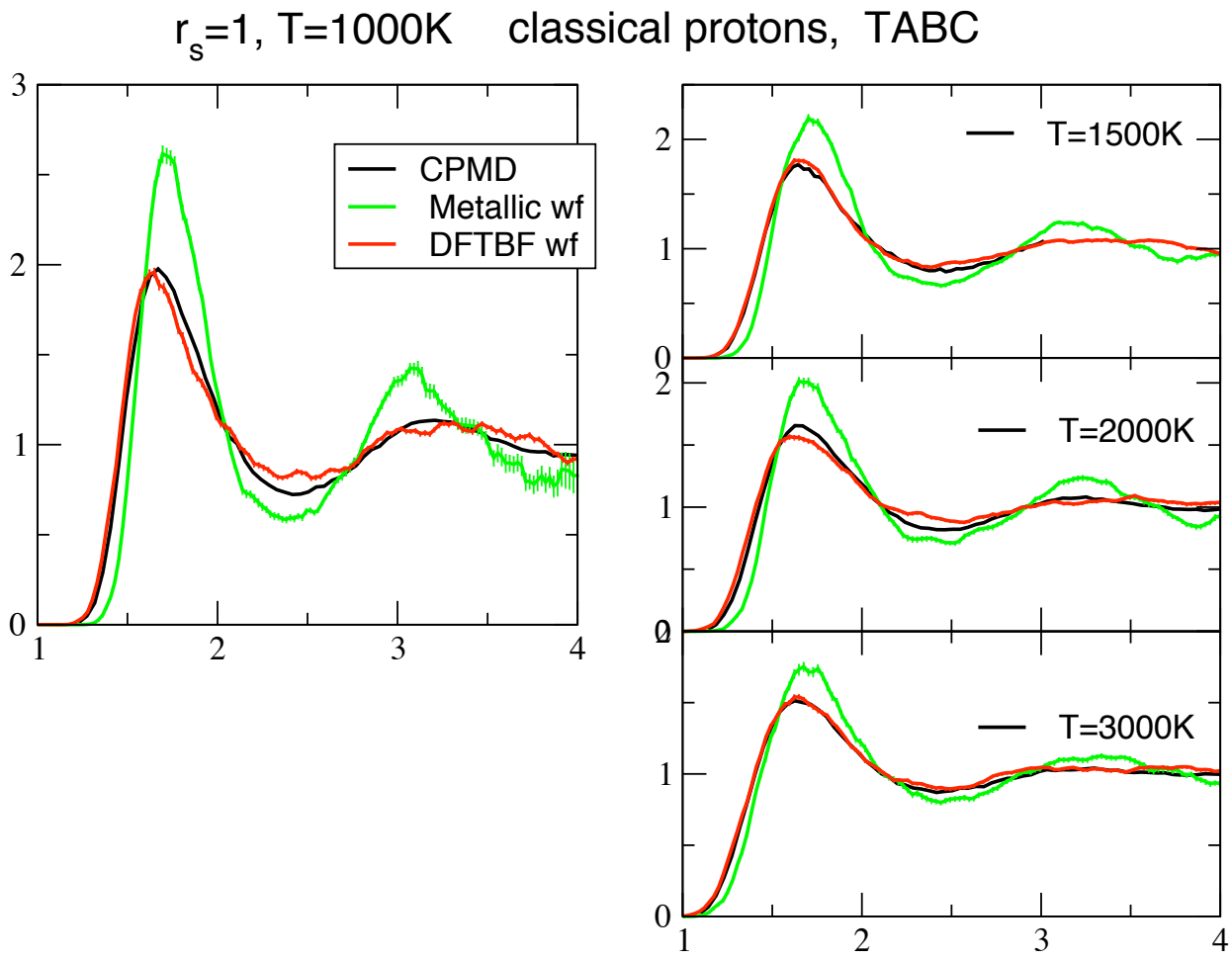

- DFTBF wf is in good agreement with CPMD data but not with the Metallic wf.
- We don't expect RQMC to change the picture.

Metallic: Pierleoni, Ceperley, Holzmann 2004

CPMD: Kohanoff Hansen 1995

Liquid-liquid phase transition: CEIMC

PRL **97,** 235702 (2006)

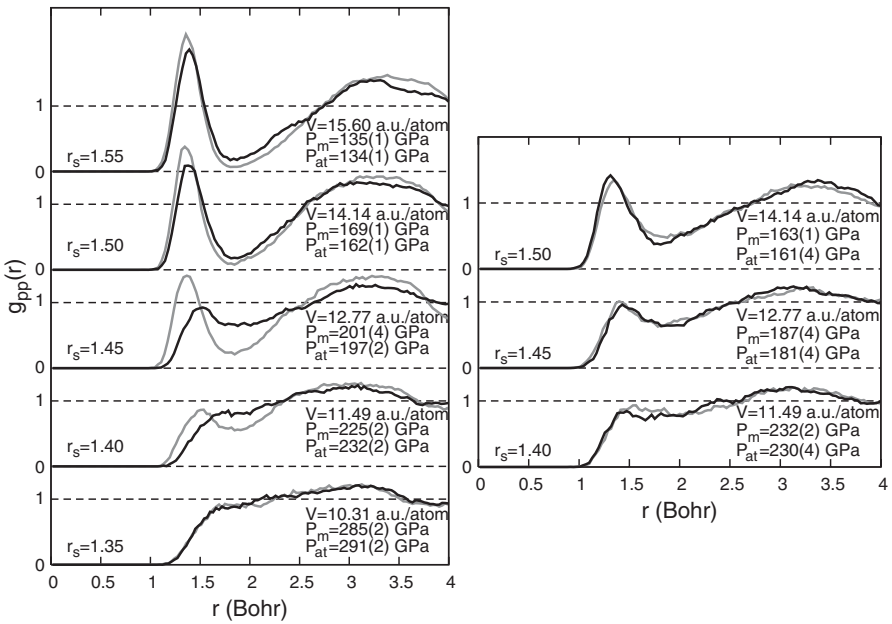

FIG. 2. Proton-proton correlation functions for CEIMC simulations in the canonical ensemble with 32 atoms at $T = 2000$ K. The BO energies are computed with VMC (left pane) or RQMC (right pane) and the wave function is a Slater-Jastrow type with bare electron-proton bands (see text). Gray lines are simulations initially prepared with a molecular fluid and black with an atomic fluid. Hysteresis is evident. $P_{\rm at}$ and P_m are the computed pressures for simulations prepared with an atomic and a molecular fluid, respectively. All correlation functions are plotted to the same scale.

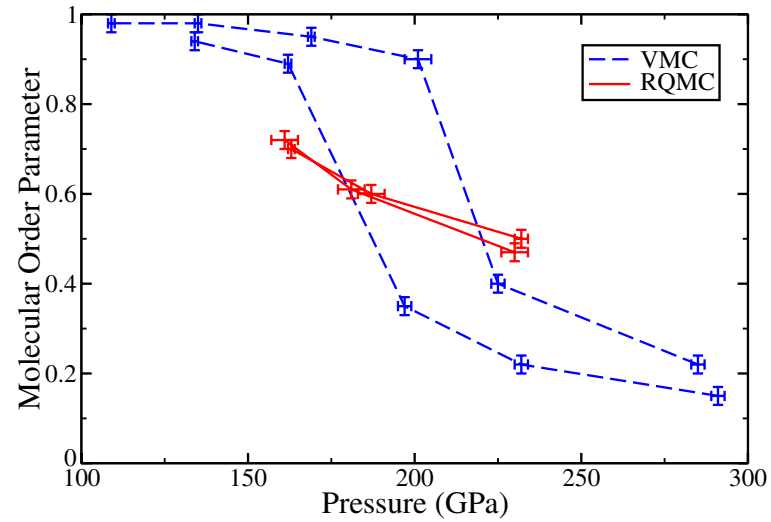

FIG. 3 (color online). Molecular order parameter [λ in Eq. (2)] evaluated for simulation results from Fig. 2. Two curves are obtained for each method from different initial conditions (see text). VMC (dashed lines) simulations indicate an irreversible, weakly first-order phase transition for molecular dissociation in the fluid with increasing or decreasing pressure. This picture is compatible with conclusions from CPMD DFT-LDA. Accurate RQMC (solid lines) simulations find a reversible crossover.

$$g(r) = \lambda g_m(r;\{\alpha\}) + (1-\lambda) g_{\rm at}(r;\{\gamma\}), \qquad (2)$$

Delaney, Pierleoni, Ceperley 2006

Liquid-liquid phase transition: CEIMC

- Simulation details
  - 32 and 54 protons at NVT conditions (T=1500K and 2000K)
  - Slater determinant with band orbitals
  - 216 twists
  - classical protons
- Main conclusions
  - at the VMC level a clear hysteresis is observed signaling the presence of metastable states: first order phase transition?
  - qualitative agreement with CPMD (Scandolo)
  - at the RQMC level the hysteresis goes away: continuous molecular dissociation
  - qualitative agreement with BOMD(GGA) at NVT conditions where a continuous molecular dissociation is observed (Vorberger et al. 2007, Holst et al. 2008)
  - VMC exhibit large size effects
  - no size effects are detected at the RQMC level

.... but ....

what will it happen at NPT conditions....
.... for quantum protons ?

melting of the atomic crystal: in progress

Atomic hydrogen: R_s=1.31, N_p=64

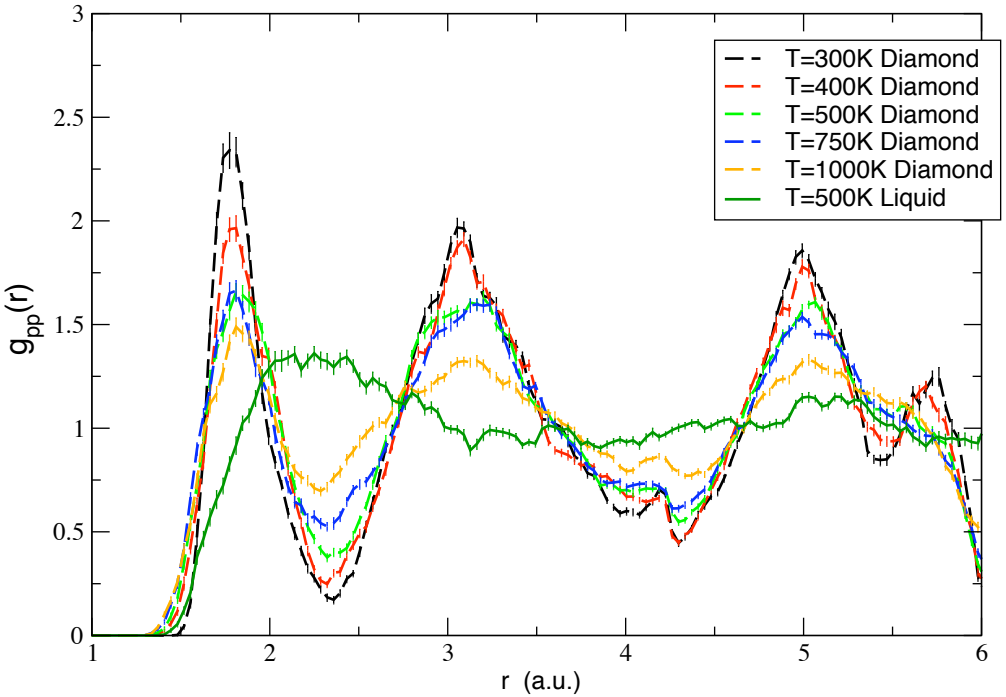

Atomic hydrogen: R_s=1.31, N_p=64

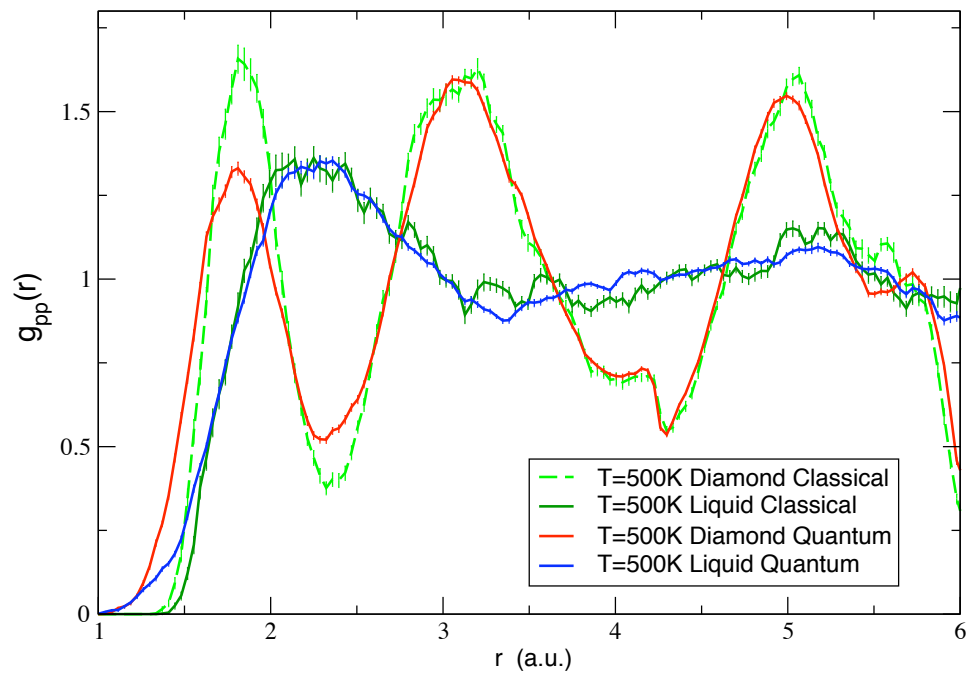

- Crystal energies are lower than corresponding liquid energies.
- Quantum protonic kinetic energies is sligthly larger in the liquid than in the crystal

system	E_{tot}(h/part)	$E_{kin} \times 10^3$
Diamond(cl)	-0.25483(3)	1.5833
Diamond(qu)	-0.25761(4)	2.95(7)
Liquid(cl)	-0.25359(2)	1.5833
Liquid(qu)	-0.2513(1)	3.18(4)

P~300Gpa

Still very preliminary results !!!!